New Fluorescent Porphyrins with High Two-Photon Absorption Cross-Sections Designed for Oxygen-Sensitization: Impact of Changing the Connectors in the Peripheral Arms

Limiao Shi, Zhipeng Sun, Nicolas Richy, Olivier Mongin, Mireille Blanchard-Desce, Frédéric Paul, Christine Odile Paul-Roth

New Fluorescent Porphyrins with High Two-Photon Absorption Cross-sections designed for Oxygen-Sensitization: Impact of changing the Connectors in the Peripheral Arms

Limiao Shi,[a] Zhipeng Sun,[a] Nicolas Richy,[a] Olivier Mongin,[a] Mireille Blanchard-Desce,[b] Frédéric Paul,[a] Christine O. Paul-Roth[a,*]

[a] Univ Rennes, INSA Rennes, CNRS, ISCR (Institut des Sciences Chimiques de Rennes) – UMR 6226, F-35000 Rennes, France.
[b] Univ. Bordeaux, Institut des Sciences Moléculaires (CNRS UMR 5255), 33,405 Talence, France
* Correspondence: author: christine.paul@univ-rennes1.fr or christine.paul@insa-rennes.fr
tel : (+33) (0) 2 23 23 63 72

ABSTRACT: In the continuation of our sustained interest for porphyrin-based dendrimers and their use as luminescent photosensitizers for two-photon photodynamic therapy (2P-PDT), we wondered about the effect of changing the connectors in our macromolecular structures. We also wanted to initiate preliminary studies on *meso*-tetraarylporphyrins decorated with more electron-releasing arms. Thus, various *meso*-tetrafluorenylporphyrin-cored star-shaped and dendrimeric derivatives have been synthesized and characterized, as well as their zinc(II) complexes. In the new dendrimeric derivatives, the peripheral fluorenyl units of the dendrons are linked to inner core either by *N-phenylcarbazole* (C_{Cbz}) or *triphenylamine* (C_{Tpa}) connectors instead of the more classic *1,3,5-phenylene* (C_{Ph}) linkers previously used by us. Selected linear and non-linear optical (LO and NLO) properties were then determined for these compounds *via* absorption or emission studies and by two-photon excited fluorescence (TPEF) measurements. It was found that the C_{Cbz}-containing dendrimer, which has the most rigid structure, exhibits a significantly lower two-photon absorption (2PA) cross-section than its C_{Tpa} analogue, presenting a more flexible structure, while rather similar luminescence and singlet oxygen activation quantum yields are found for both of them. The origin of this unexpected discrepancy is briefly discussed, based on our photophysical data. It is then demonstrated that the latter dendrimer also outperforms several closely related dendrimers in terms of 2PA action cross-section and 2PA-oxygen sensitization, making its molecular architecture quite appealing for developping new 2PA photosensitizers suited to theranostic uses.

Keywords: Porphyrin • Fluorenyl • Phenyl • Carbazole • Triphenylamine • Two-Photon Absorption • Oxygen Sensitization

Introduction

Nowadays porphyrin-based systems are foreseen as key building blocks for many applied developments because they present remarkable photochemical and redox properties which can be fine-tuned by modification of the peripheral substituents. Consequently, impressive fundamental research based on porphyrins has been undertaken in fields related to material sciences and information treatment,[1–2] but also in fields related to health, such as photodynamic therapy (PDT) for instance.[3] In this particular field, their use as photosensitizer (PS) for PDT has been revived subsequent to the observation that oxygen sensitization might advantageously be triggered by two-photon absorption (2PA-PDT), since this kind of excitation (usually conducted at energies in the near infrared domain) affords a deeper penetration in living tissues, less photodamages and permits an exquisite spatial control (around the focal point of the laser) with minimal autofluorescence.[4] The last point is especially important when the two-photon PS can also be coupled to a fluorescent probes, allowing to perform curing and imaging at the same time in a so-called theranostic approach.[5–6] Given that *meso*-tetraphenylporphyrin (**TPP**) is only modestly fluorescent in its free base form (Φ_F = 11%) and present a rather weak two-photon absorption cross-

section (σ_2^{max} = 11 GM), most of the investigations in this field relied on porphyrin derivatives featuring an expanded (star-shaped or dendritic) π-manifold, in order to enhance the 2PA cross-section and also to boost their two-photon action cross-section (sometimes called two-photon brilliancy).[7]

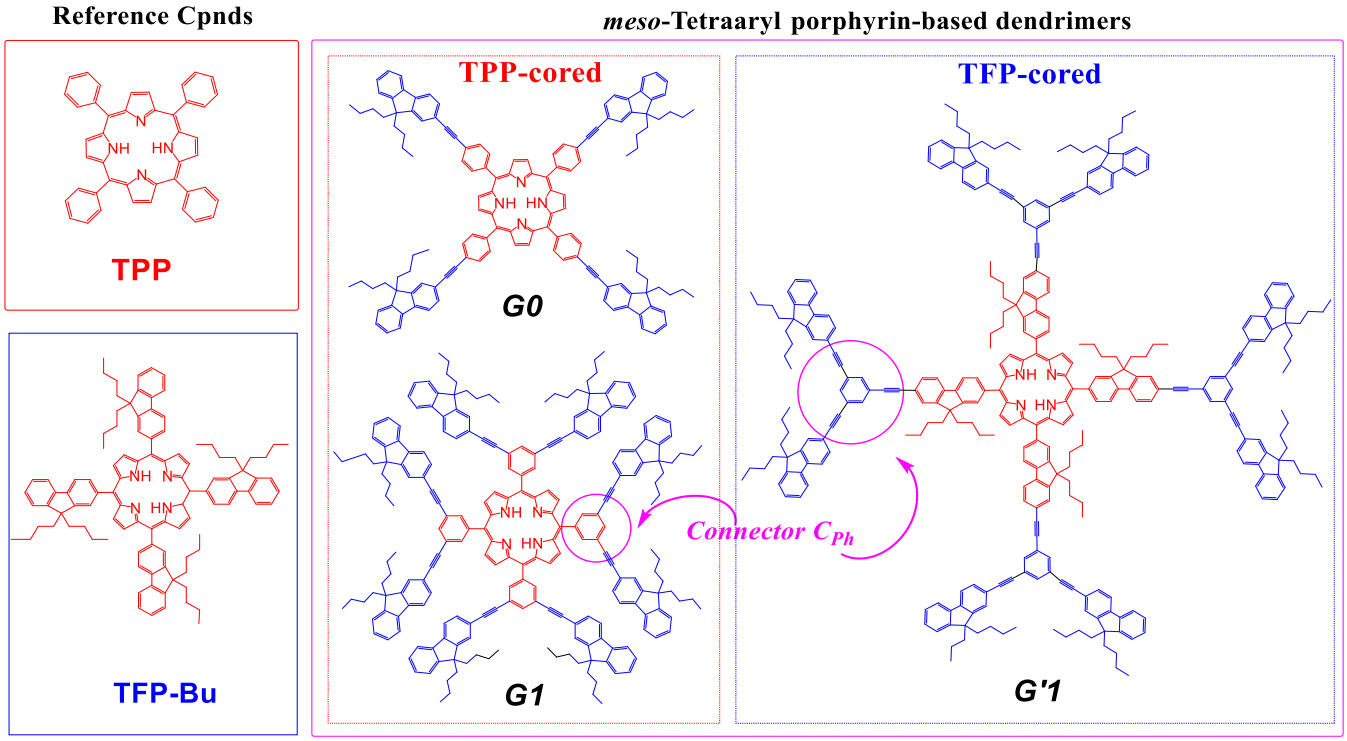

Scheme 1. Molecular structures of increasing generations (***G0*** to ***G1***) of **TPP**-based dendrimers with peripheral fluorenyl-branched arms *via* a "***C*$_{Ph}$**" Connector and **TFP**-cored analogue of ***G1*** (***G'1***).

This expansion was often performed *via* alkynyl or alkenyl linkers appended at the *meso*-positions of the porphyrin ring.[4,7] This was usually accompanied by a red-shift of the porphyrin absorptions at lowest energy, strongly reducing the spectral window available for two-photon excitation (2PE). At difference with such approaches, we could recently show with various families of *non-conjugated*-[8–10] or *semi-disconnected* dendrimeric porphyrins (Scheme 1),[11–12] that by appending *fluorenyl-containing dendrons* at the periphery of a central tetra-arylporphyrin core, fluorescent PS, with significantly enlarged one-photon brightnesses and 2PA cross-sections, could be obtained.

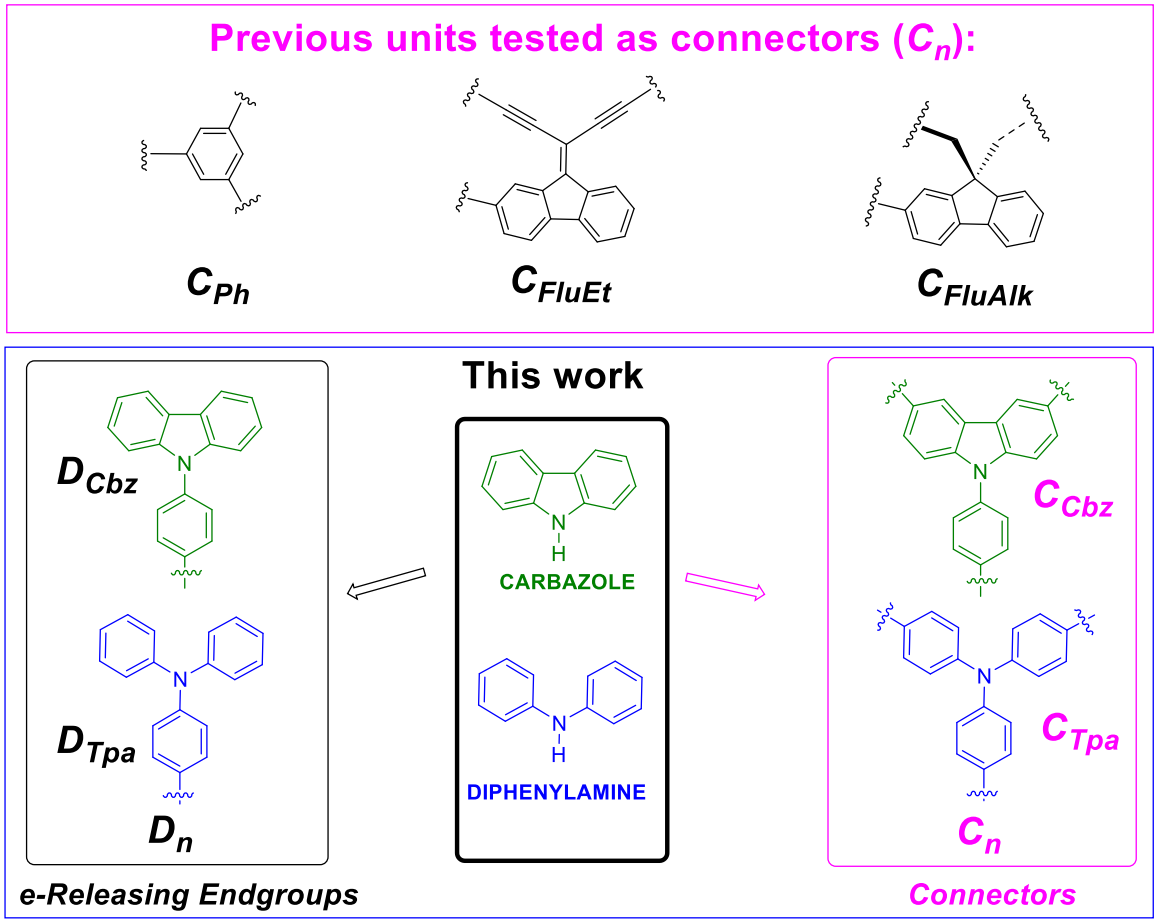

Scheme 2. Molecular structures of various connectors previously used and of carbazole and di/triphenylamine, used as either donor end-groups (D_n) or connectors (C_n).

By replacing the central **TPP** core by tetrafluorenylporphyrin (**TFP**), a porphyrin possessing four 2-fluorenyl arms,[14] dendrimers with doubled fluorescence quantum yields can even be obtained.[12] The **TFP** core not only increases the luminescence, but also the singlet oxygen formation quantum yield (Φ_Δ = 60%).[8] Thus, each of the desired properties was significantly improved in ***G'1*** compared to its **TPP**-cored analogue ***G1***.[12] In all these compounds, the well-known *1,3,5-phenylene* unit (C_{Ph}) was always used as branching unit in the dendrons. However, such a linker allows only a weak (if any) electronic communication between the *meta*-phenyl positions to which the fluorenyl-containing antennas are appended, a feature which we thought could be detrimental to 2PA. In the hope of improving further their properties, we have then decided to test other connecting units and to study their impact on the optical properties of interest.So far, only two 9,9′-bifunctionalised fluorenyl units (C_{FluEt} and C_{FluAlk} in Scheme 2) were tested as substitutes for C_{Ph} in such compounds. While the former (C_{FluEt}) turned out to be significantly more efficient than C_{Ph}, the synthesis of these compounds was however much more challenging.[13] Now, other alternative connectors can also be considered in our dendrons such as triarylamines[15–16] or *N*-functionalized carbazoles.[17,19] These aromatic amines were already used as branching units (or "connectors") in emissive carbon-rich dendrimeric assemblies (Scheme 3), some of which exhibited also significant two-photon absorption properties.[15–17]

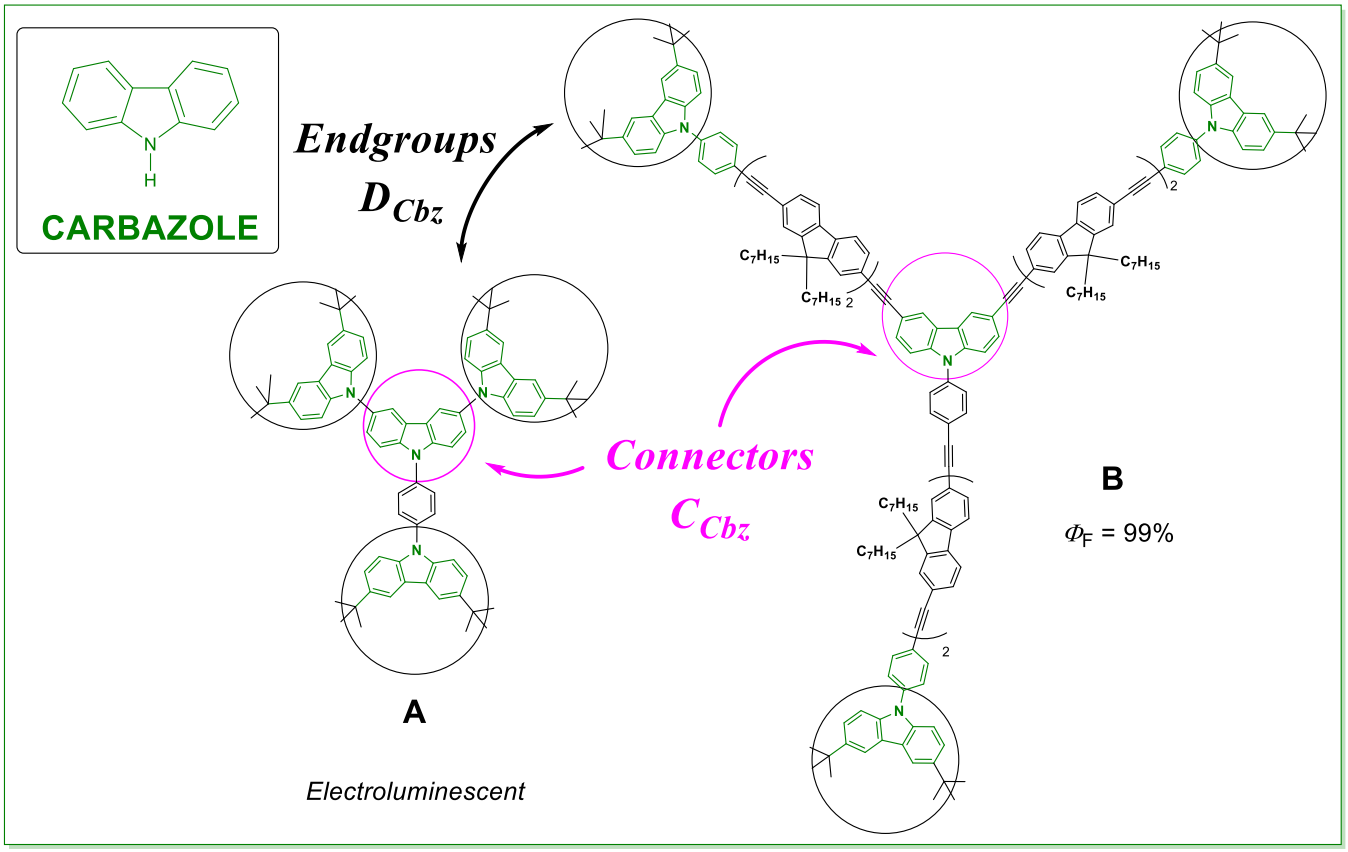

Scheme 3. Selected examples of a *carbazole* derivative **A**[18] and of a *carbazole/fluorene* compound **B**.[19]

Furthermore, beside their use as a connector, triarylamine units are often used as electron-releasing end-groups in various molecules designed for 2PA.[20–21] In this respect, the role of the *N*-phenyl carbazole unit is comparably less well established.[22–23] Although this more rigid unit could in principle lead to a better overlap between the *N*-phenyl and the carbazole π-manifolds, a desirable feature for 2PA, until yet, as an endgroup it was mostly used to develop electroluminescent polymers rather than NLO-active dendrimers.[23–24]In order to learn more about the potential of these units to develop fluorescent photosensitizers similar to ***G'1***, we will now synthesize a set of four **TFP**-cored compounds (Scheme 4) featuring ***N-phenylcarbazole*** (***C***$_{Cbz}$) or ***triphenylamine*** (***C***$_{Tpa}$) units, either as electron-releasing endgroups (named ***D***$_{Cbz}$ or ***D***$_{Tpa}$, respectively) in the related star-shaped derivatives (**1** and **2**), or as connectors, in *generation-1* dendrimers similar to ***G'1*** (**3** and **4**). In addition, their Zn(II) complexes (**5**-**8**) will also be isolated and characterized.

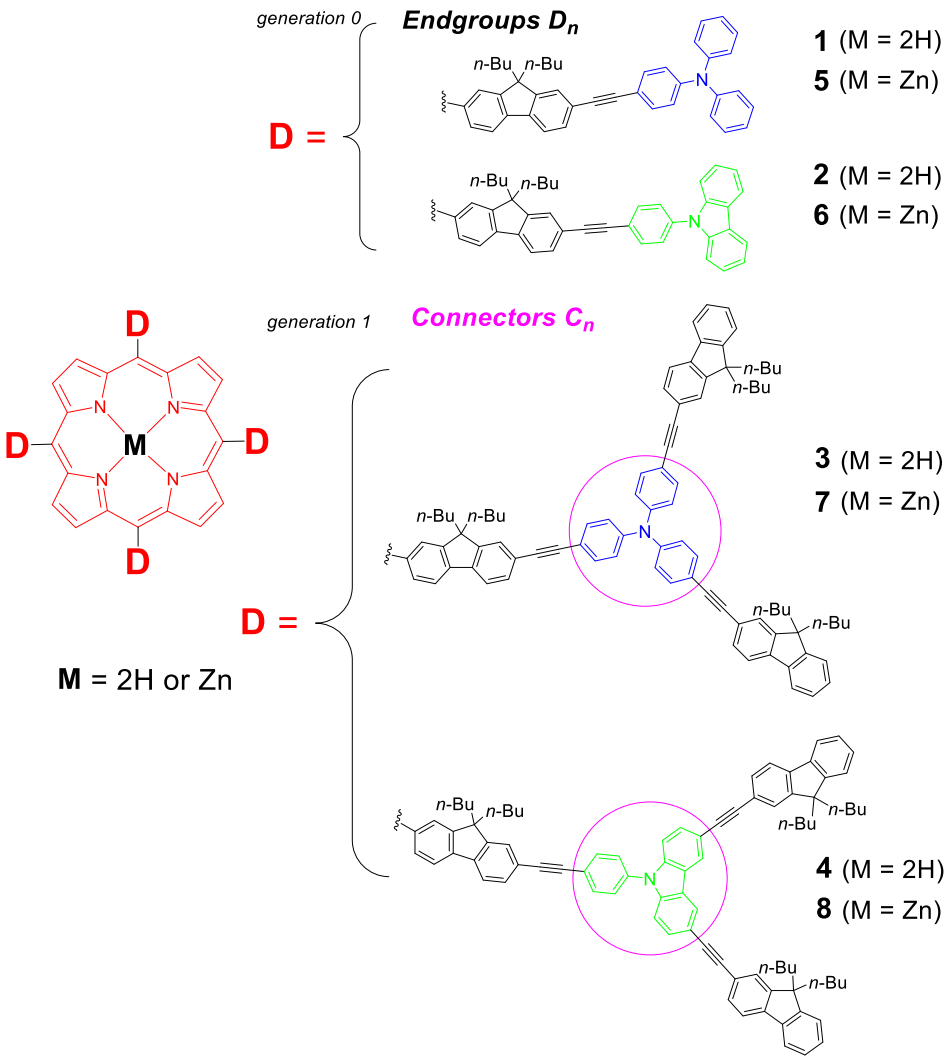

Scheme 4. Molecular structures of target **TFP**-cored free-base dendrimers of generation-0 (**1-2**) and generation-1 (**3-4**), and of their Zn(II) complexes (**5-8**).

The study of their photophysical properties will then be performed and they will be compared to those of known dendrimeric analogues such as ***G'1***[12] and related compounds.[3,7,22] During this work, the compounds featuring these units as endgroups (**1** and **2**) will help us benchmarking the purely electronic effect of these connectors on the central **TFP** core, while the study of compounds **5-8** will then help us to delineate more precisely the role of the zinc(II) on the relevant photophysical properties of interest for developing fluorescent 2PA-photosensitizers.

Results

Syntheses of the Targeted Dendrimers.

The desired free-base porphyrins (**1–4**) were were obtained by condensation between the corresponding aldehyde and pyrrole under soft Lindsey conditions (Scheme 5).[25,26] Their zinc complexes **5-8**, were then obtained by reaction between these porphyrins and zinc acetate.[27] First we will describe the synthesis of the precursor aldehydes **9-12** of the peripheral arms and then of the synthesis of the various porphyrins (**1-8**).

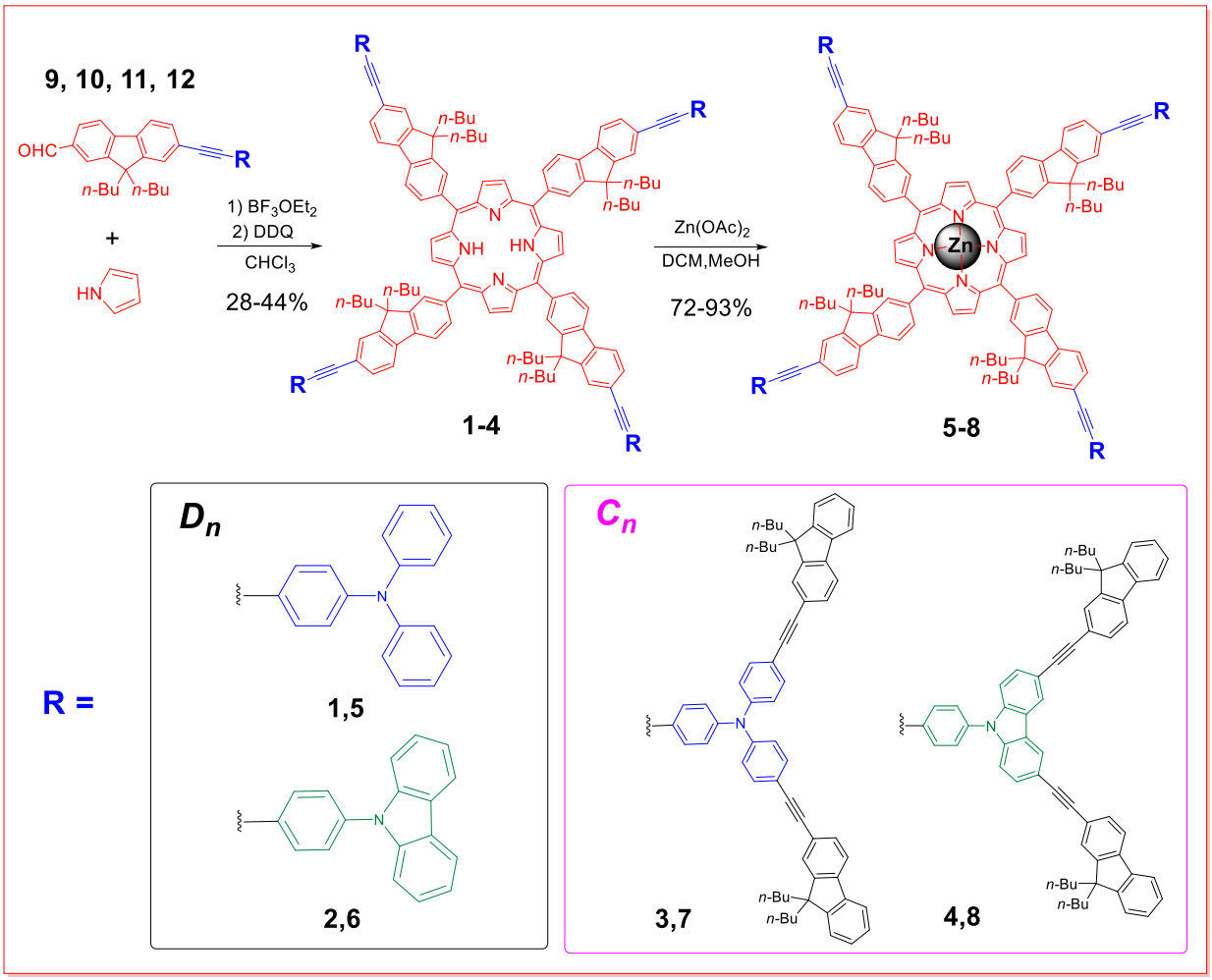

Scheme 5. Synthesis of free-base porphyrins (**1-4**) and the corresponding Zn(II) complexes (**5-8**).

Synthesis of linear fluorenaldehydes 9 and 10. The two aldehydes with a diphenylamine (**9**) or a carbazole (**10**) endgroup, are both accessible in four steps from commercial reagents (ESI). Only the last step is reported here for sake of conciseness.

The fluorenaldehyde **9** was obtained by coupling alkyne **13**[28,29] with the bromofluorene derivative **14**[12] under harsh Sonogashira conditions.[30] This reaction proceeded over two days at 100°C, in a diisopropylamine ($^{i}Pr_2NH$) and *N,N*-dimethylformamide (DMF) mixture in the presence of the palladium precatalyst ($Pd(PPh_3)_2Cl_2$) and copper iodide (CuI). The new fluorenylaldehyde **9** was obtained in 95% yield, after column chromatography on silica gel (Scheme 6).

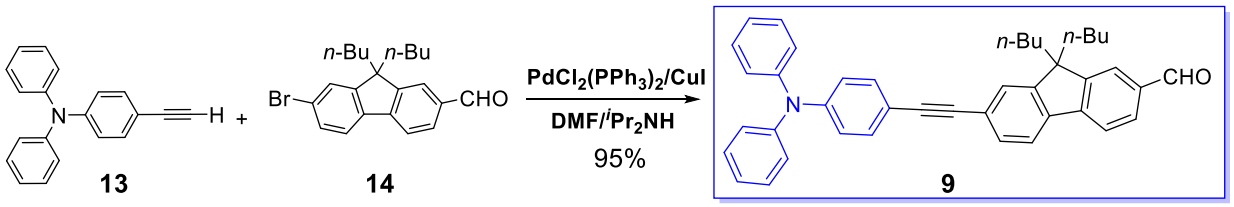

Scheme 6. Formation of fluorenylaldehyde **9** having a triphenylamine endgroup (D_{Tpa}).

The fluorenylaldehyde **10** was obtained in 51% yield using a reversed approach *i.e.* by coupling the carbazole derivative **15**,[31,32] having a 4-bromoaryl substituent, with the known[33,12] ethynyl-terminated fluorenylaldehyde **16** (Scheme 7). These reaction conditions are similar as before but a different palladium(II) precatalyst was used ($Pd(OAc)_2$).

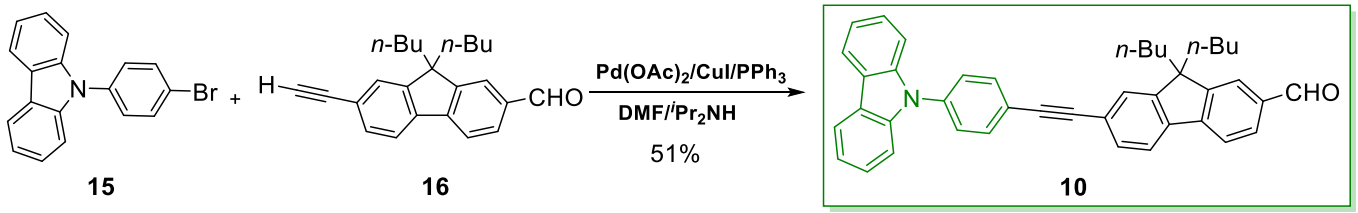

Scheme 7. Formation of fluorenylaldehyde **10** with a carbazole endgroup (D_{Cbz}).

Synthesis of fluorenaldehydes 11 and 12. These higher *generation* dendron precursors, are both accessible in five steps from commercial reagents (ESI). Again, only the last step is reported below for sake of conciseness.

The fluorenylaldehyde **11** was isolated in 63% yield after reacting the bromo-derivative **17** with the known alkyne **16**[12] under Sonogashira conditions (Scheme 8). The precursor **17** was obtained from 9,9-dibutyl-2-((4-iodophenyl)ethynyl)-*9H*-fluorene (**18**) and commercial 4-bromoaniline through a double Ullmann-type cross-coupling reaction in 80% yield (ESI, Figure S9).[31,32]

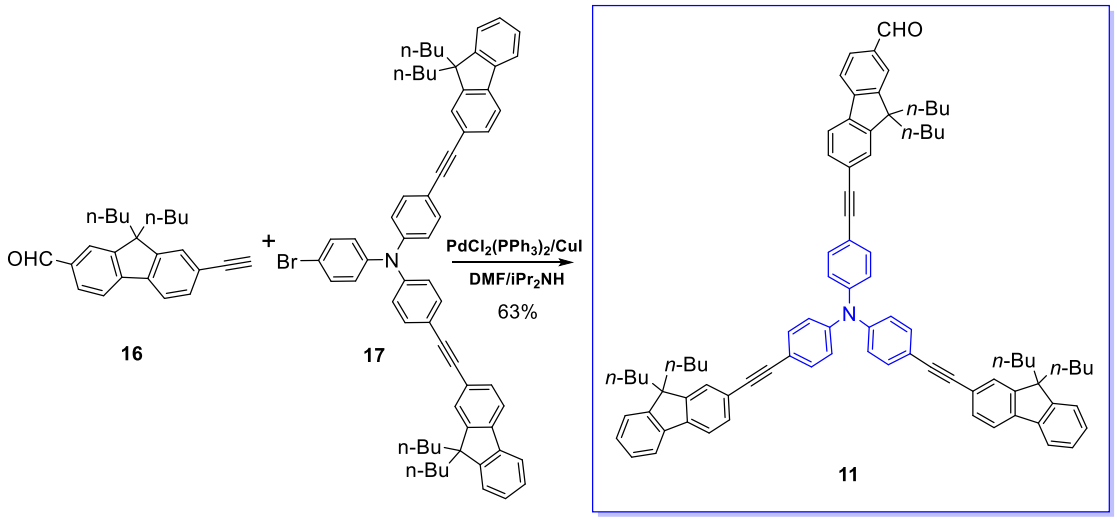

Scheme 8. Formation of dendron **11** with a triarylamine connector C_{Tpa}.

The fluorenylaldehyde **12** was also synthesized by coupling the iodo-derivative **19** and alkyne **16**[12] under conditions similar to those used for aldehyde **9**, in 33% yield (Scheme 9). The key precursor **19** was obtained in five steps from commercially available 3,6-dibromo-*9H*-carbazole, through Sonogashira coupling with ethynyltrimethylsilane followed by removal of the TMS protecting group to obtain the known bis-alkyne-carbazole intermediate **20**[34] (ESI, Figure S10).

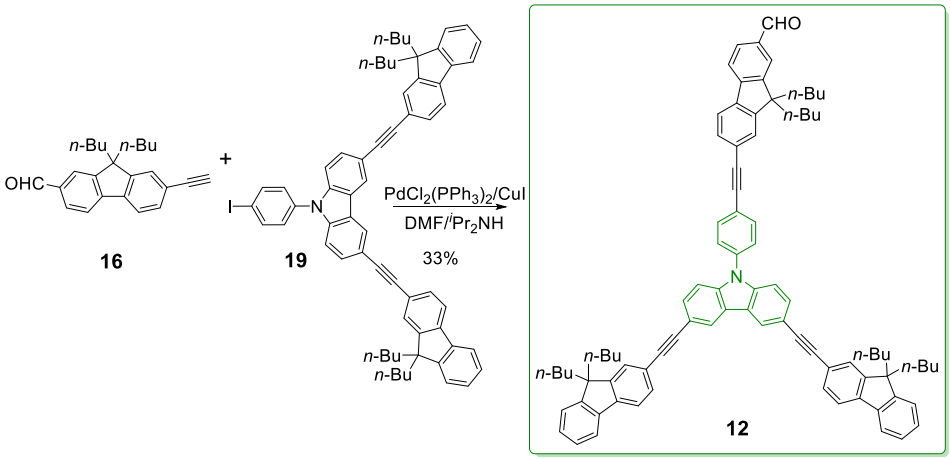

Scheme 9. Formation of dendron **12** with a carbazole C_{Cbz} junction.

Syntheses of the Porphyrins. The free-base porphyrins **1**-**4** were then synthesized by condensation of the corresponding aldehydes (**9**-**12**) with pyrrole under Lindsey's conditions,[25,26] using $CHCl_3$ as a solvent, BF_3 etherate as an acidic catalyst and DDQ as an oxidant. They were obtained pure in 42%, 44%, 28% and 36% yield, respectively (Scheme 5). The corresponding Zn(II) complexes (**5**-**8**) were obtained after metalation by zinc acetate in a mixture of dichloromethane and methanol and were isolated in 72%, 93%, 82% and 77% yield, respectively.

Characterization of the Dendrimers. After chromatographic purification and recrystallization, all new dendrons (**9**-**12**) and porphyrins (**1**-**8**) were characterized by usual techniques, including elemental analysis. Thanks to the *n*-butyl chains on the peripheral fluorene groups, they all exhibited sufficient solubilities for NMR characterization. Moreover, based on the previous investigation,[12] we know that introduction of the various *n*-butyl chains has almost no effect on their electronic structure nor on their optical properties, apart perhaps slightly decreasing their fluorescence quantum yields.[8] All compounds were then characterized by ^{1}H NMR, ^{13}C{^{1}H} NMR and HRMS or elemental analysis.

The ^{1}H NMR spectra of the starting aldehydes **9**, **10**, **11** and **12** can be divided into three parts (Figure 1): (i) one singlet for the aldehyde proton around 10 ppm, (ii) signals arising from the aromatic protons between 7 and 8 ppm, (iii) signals of the aliphatic protons of the *n*-butyl chains around 0.5-2.2 ppm. A comparison of the detailed spectra of the four aldehydes (**9**, **10**, **11** and **12**) is given in Figure 1. The singlet around 10 ppm belongs to the aldehyde proton (-C*H*O); and there are many aromatic peaks around 7-8.5 ppm, but we notice that the singlet (H_B) of the phenyl ring of dendron **11** in the carbazole series, can be distinguished. It integrates in total for eight protons, as does the doublet H_A of the phenyl ring of compound **10**. Notably, the singlet belonging to proton H_B in **11** appears at lower field than the H_A proton in **10**, because the dendron **11** presents a longer conjugated system than **10**. The alkyl protons, of the *n*-butyl chains on the fluorenyl units, are localized between 0 to 2.2 ppm and are separated into four multiplets (H_a, H_b, H_c and H_d) as seen in Figure 1.

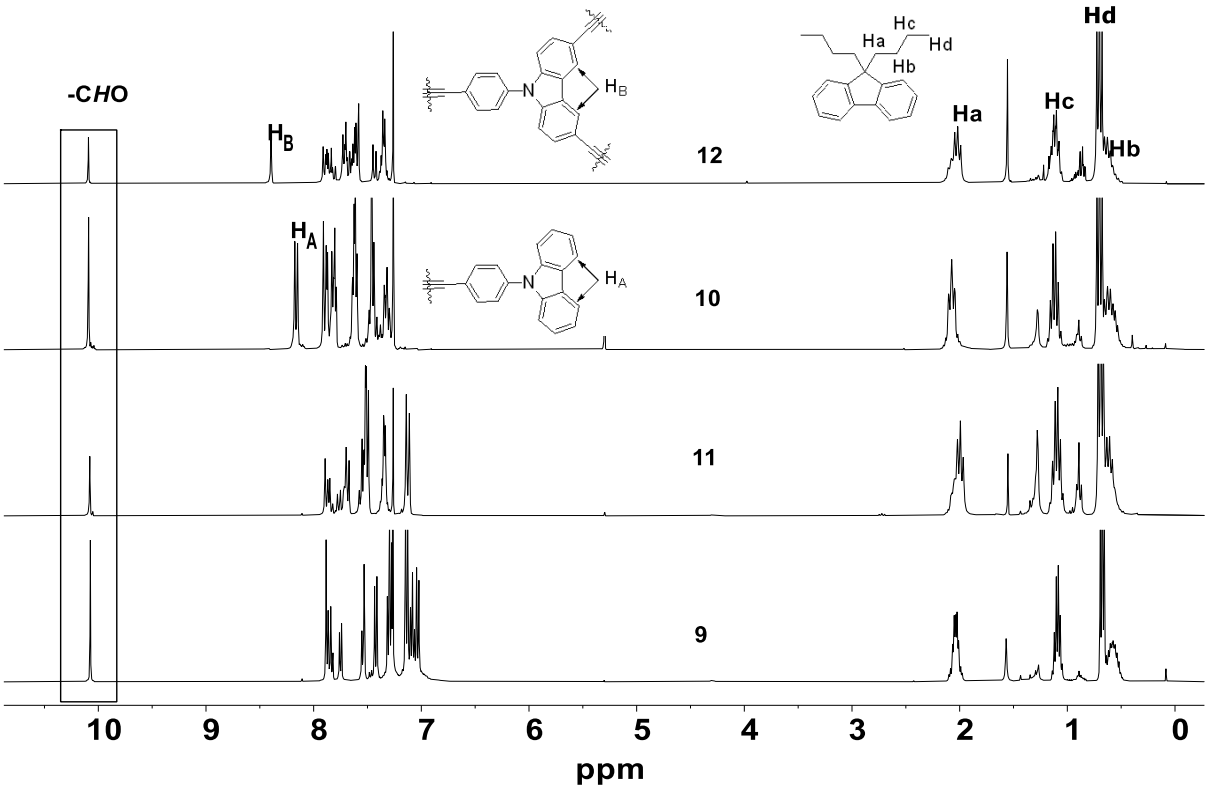

Figure 1. Detailed ^{1}H NMR spectra of aldehydes **9**-**12**.

For the ^{1} H NMR studies of the porphyrins, we will consider the *triphenylamine* series and *carbazole* series separately:

The spectra of porphyrins **1**, **3**, **5** and **7** belonging to the *triphenylamine* series are shown in Figure 2 (for more details, see ESI; Figure S14). Their spectra can be subdivided in four parts: (i) the β-pyrrolic protons region (H_β) near 9 ppm, (ii) the aromatic region between 7.0 and 8.5 ppm, (iii) aliphatic region showing the *n*-butyl chain protons around 2.2-0.5 ppm

and (iv) the region around -2.6 ppm corresponding to –N*H* protons inside the macrocyclic cavity (for the free-base porphyrins only).

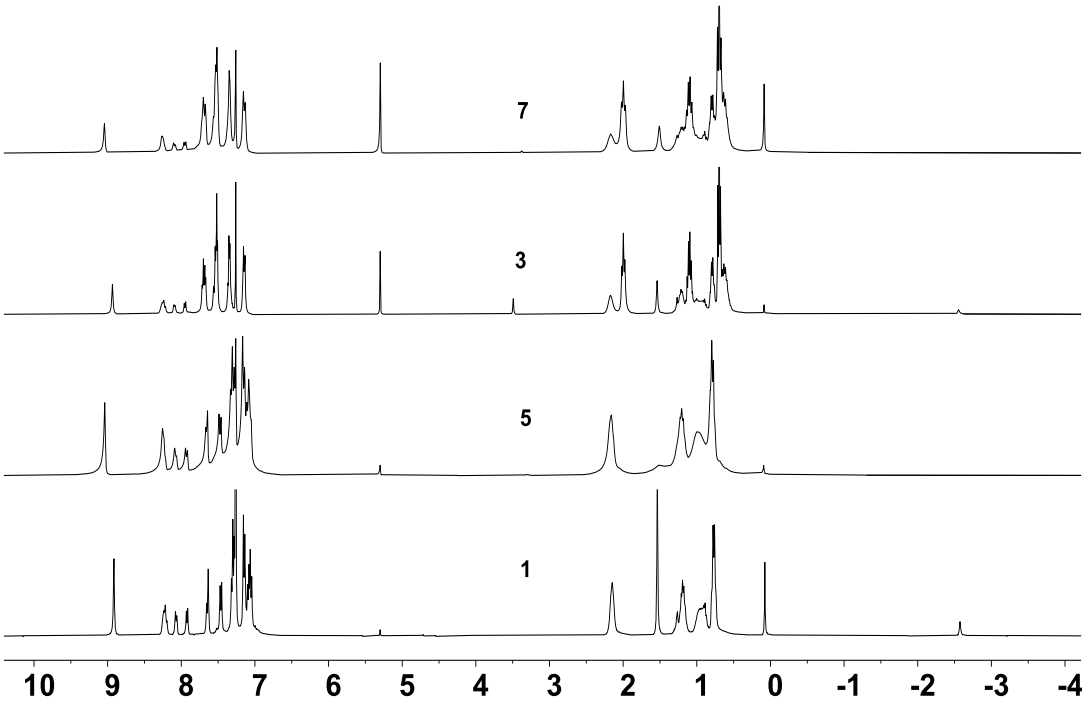

Figure 2. Complete ^{1}H NMR spectra of the *triphenylamine* porphyrin series (**1**, **3**, **5** and **7**).

The spectra of porphyrins **2**, **4**, **6** and **8** belonging to the *carbazole* series have also four diagnostic sets of signals (regions i-iv) for free-bases **2** and **4**, and only three (i-iii) for the Zn(II) complexes **6** and **8** (see ESI ; Figure S15 for a more detailed assignment).

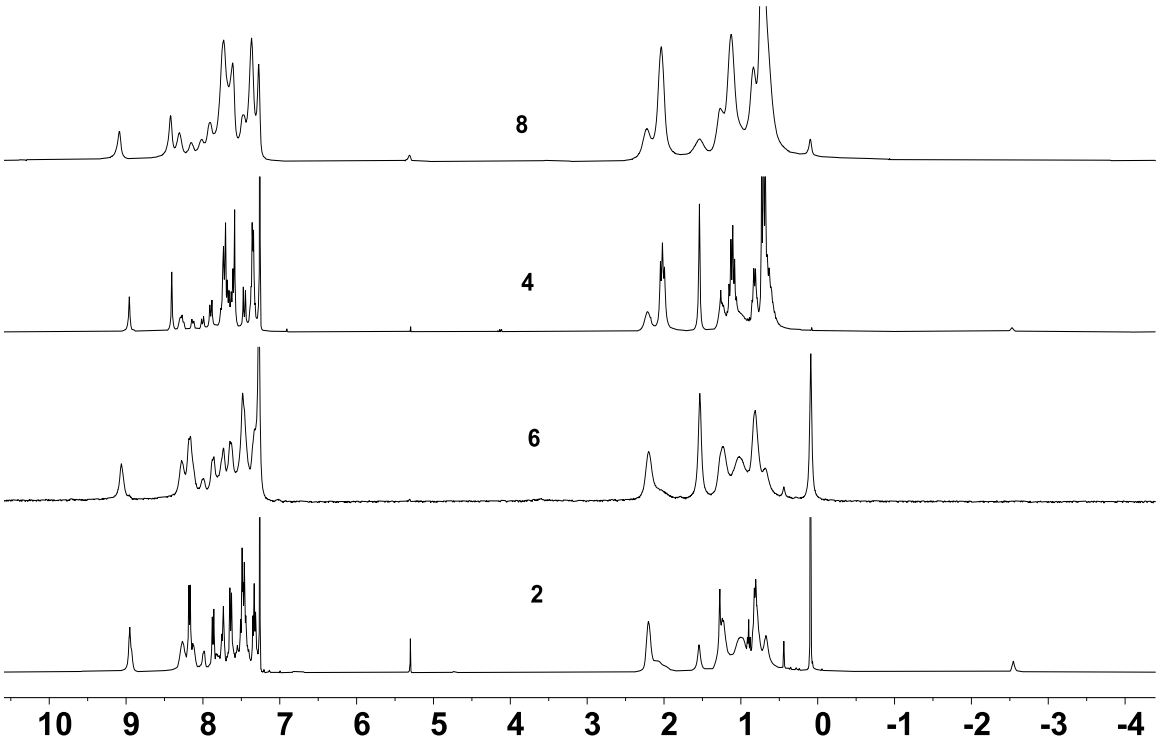

Figure 3. Complete ^{1}H NMR spectra of the *carbazole* porphyrin series (**2**, **4**, **6** and **8**).

Optical Properties. One- and two-photon absorption (1PA and 2PA) and emission properties, as well as oxygen photosensitization properties were next determined for **1-8** in CH_2Cl_2 solution, using **TFP-Bu** as reference (Tables 1 and 2).

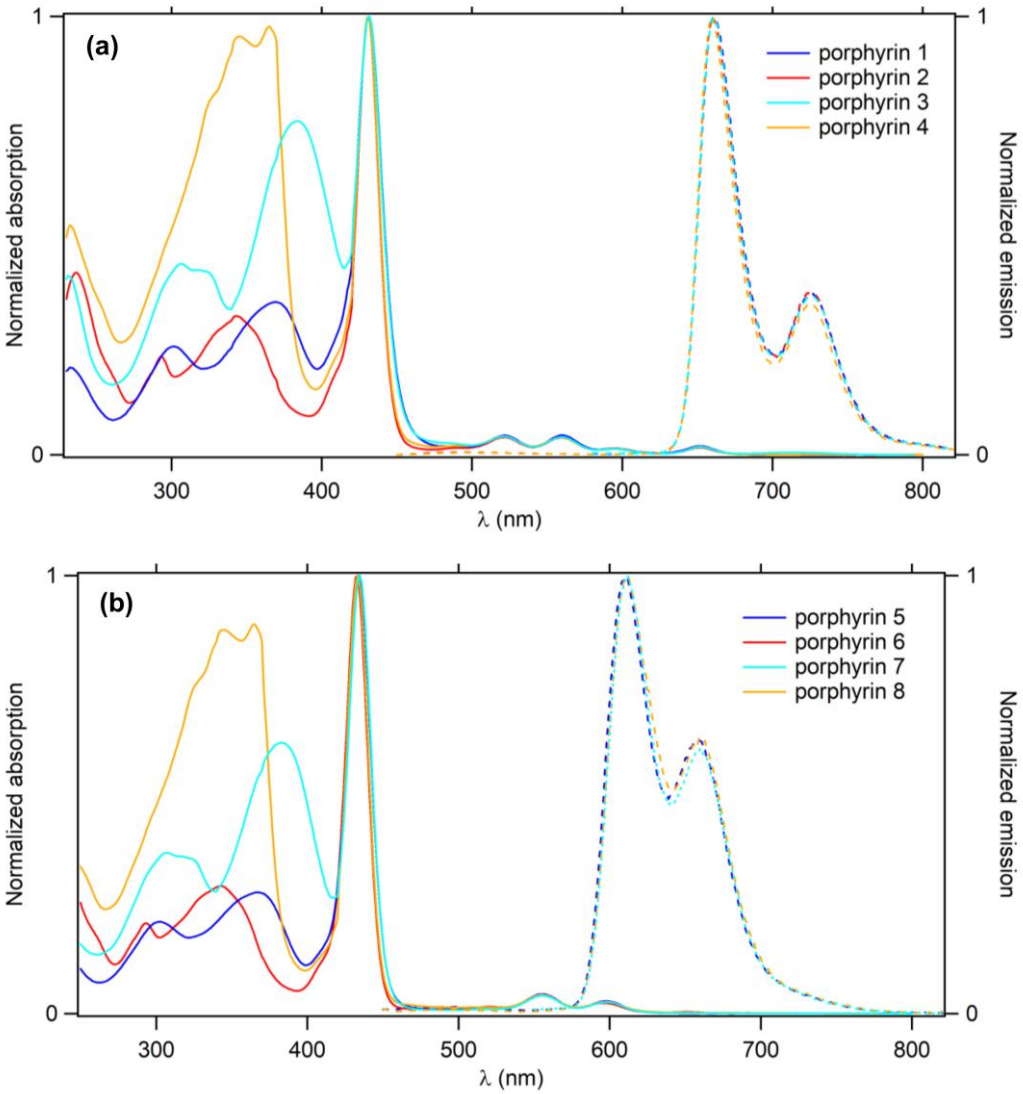

Figure 4. *UV*-visible absorption and emission spectra in CH_2Cl_2 of (a) the free-base porphyrins **1**-**4** and (b) their Zn(II) complexes **5**-**8**.

Absorption spectra. The UV/Vis absorption spectra of all these new porphyrins were recorded between 250 and 820 nm (Figure 4). Without surprise, the spectra of the latter have three components: (i) a broad dendron-centered band at around 280-400 nm, which corresponds to a $\pi \rightarrow \pi^*$ transition; (ii) a Soret-band around 430-435 nm and (iii) four typical Q absorption bands around 500-660 nm for the free-base porphyrins (Figure 4a). As expected, instead of these four Q-bands, the zinc complexes give only two Q-bands around 555-598 nm (Figure 4b).

A closer examination of these absorption spectra (Figure 4a) reveals that for the *triphenylamine* series (blue lines), the absorption spectra profiles of free-base porphyrin **1** and of its higher generation analog **3** are almost identical. This is also true for porphyrin **2** and its higher generation analog **4** in the *carbazole* series (red-orange color). However, after normalizing the spectra on the intensity of the Soret-band, the dendron absorption significantly increases with increasing dendrimer generation. Thus, for both series, we can notice a strong hyperchromic shifts of the band close to the blue edge of the spectra, in agreement with a more extended π-system in the *generation-1* dendrimers. The porphyrin-based transitions (Soret-band and Q-bands) are not shifted and maintain constant intensities as the dendrimer generation

increases. For all these free-base porphyrins, the Soret-band is at slightly higher energy than for their Zn(II) complexes (431 *vs.* 435 nm). The replacement of triarylamine units in **1** and **3** with carbazole units (**2** and **4**) leads to a hypsochromic shift (~20 nm), suggesting that the conjugation through triarylamine is more efficient than through carbazole (Table 1).

Table 1. Photophysical properties of complete series **1-8** in CH_2Cl_2.

Cmpd	λ_{abs} **Dendron** (nm)	λ_{abs} **Soret** (nm)	ε **Soret** (10^3 M^{-1} cm^{-1})	λ_{abs} **Q bands** (nm)	λ_{em}(nm) **Q(0,0)**	**Q(0,1)**	Φ_F[a]
TFP-Bu	-	427	-	519,555,596,652	659	725	0.20
1	370	431	479	521,560,595,652	661	726	0.21
2	343	431	536	521,559,594,652	660	726	0.20
3	306,384	431	610	522,561,594,632	661	726	0.19
4	365	431	518	521,559,595,652	660	726	0.20
5	303,366	434	569	556,598	611	657	0.09
6	343	433	543	555,596	-	-	-
7	307,383	435	661	555,598	612	660	0.09
8	345,365	433	544	555,598	611	660	0.09

[a] Fluorescence quantum yield determined relative to **TPP** in toluene.

Emission spectra. Upon excitation at their Soret-band, the free-base porphyrins (**1**-**4**), and the reference porphyrin **TFP-Bu**[8] exhibit the two characteristic porphyrin emission peaks Q(0,0) and Q(0,1) at 660 and 726 nm (Table 1). After normalizing the emission intensities of the various porphyrins on their Q(0,0) peaks, the four new porphyrins exhibit similar emission spectra (Figure 4a) and the intensity ratios between Q(0,0) and Q(0,1) remain constant. With respect to emission quantum yields, these TFP-cored porphyrins (**1**-**4**) resemble the reference compound **TFP-Bu**, so that their emission quantum yield remains very high for *meso*-tetra-arylporphyrin derivatives (19-21%).

For zinc porphyrins, the four complexes (**5**-**8**) exhibit also similar emission spectra (Figure 4b), with constant intensity ratios between Q(0,0) and Q(0,1) bands. A notable difference with free-base porphyrins is the significant blue-shift of the emission maximum wavelength, Q(0,0) from 660 nm to 611 nm, and Q(0,1) from 726 nm to 660 nm. While all Zn(II) porphyrins show similar fluorescence quantum yields (~9%), these are lower than the parent free-base porphyrins, but nevertheless three times higher than **ZnTPP** (3%).[8] Thus, these quantum yields are not affected by the dendrimer generation.

The ***energy transfer (EnT)*** from peripheral dendrons towards the central porphyrin core was also evaluated in CH_2Cl_2 solutions at 20 °C. Figure 5 shows the emission spectra of the free-base porphyrins and Figure S16 (ESI) shows those of the corresponding zinc porphyrin complexes. Upon excitation at the dendron absorption (340~390 nm), the emission spectra of the free-base porphyrins show a set of red emission peaks characteristic of the porphyrin core (at 660 and 726 nm) plus a residual blue emission, characteristic of the dendrons (around 480 nm). This dual emission reveals that the corresponding $\pi \rightarrow \pi^*$ excited state is not totally quenched by EnT to the central porphyrin core. Porphyrins **1** and **3** (blue lines) feature the most intense dendron-based emission suggesting that EnT from the donor conjugated dendrons to the porphyrin acceptor core (Scheme 10) is less efficient through C_{Tpa} than through C_{Cbz} (red-orange lines), but this is not more so marked when the energy transfer quantum yields are derived using the starting aldehydes **9-12** as models for the dendrons in **1-4** (ESI). Quantum yields between 94% and 98% are actually found for these compounds, suggesting a nearly quantitative EnT in all cases. Notably, such behavior was not observed for the free-base analogue **G'1** featuring 1,3,5-phenylene spacers C_{Ph} for which the quenching of the dendron-based emission was total, pointing toward some detrimental influence of the connector/endgroup of the peripheral arms on this process in **1-4**, since, most likely, this energy transfer proceeds via a through-bond mechanism (TBET).[35] This has perhaps to do with the larger electron-richness of C_{Tpa} and of C_{Cbz} compared to C_{Ph} (see discussion section). Very similar energy transfer quantum yields (95-96%) are found for the Zn(II) porphyrins **5**-**8** for which the dendron-based emission is also not completely quenched by EnT indicating that zinc plays a minor role in this process.

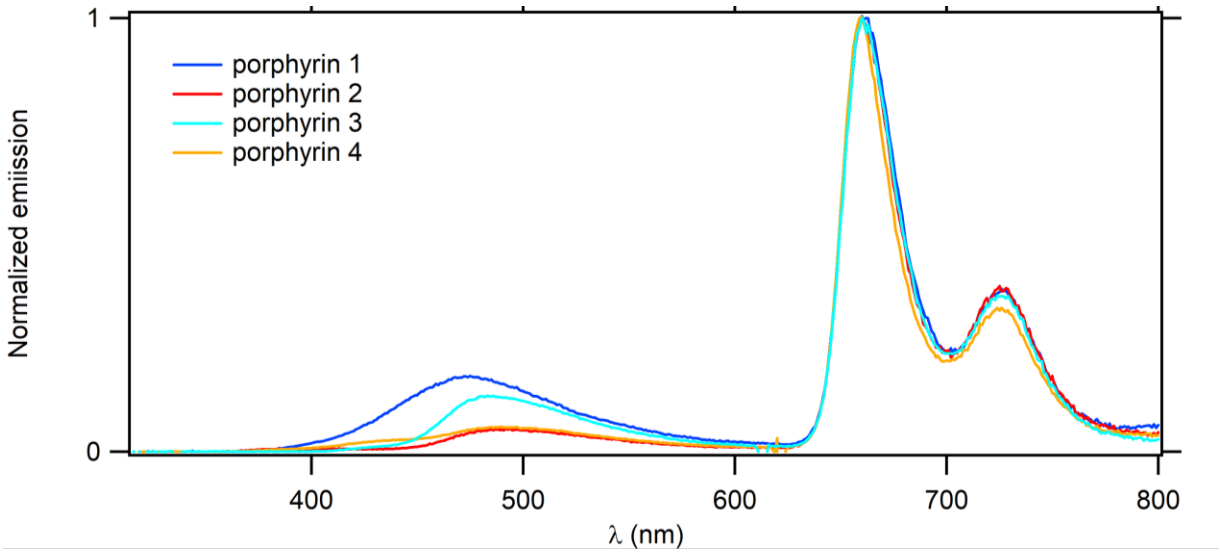

Figure 5. Emission spectra upon UV excitation at fluorenyl band for free-base porphyrins (**1-4**).

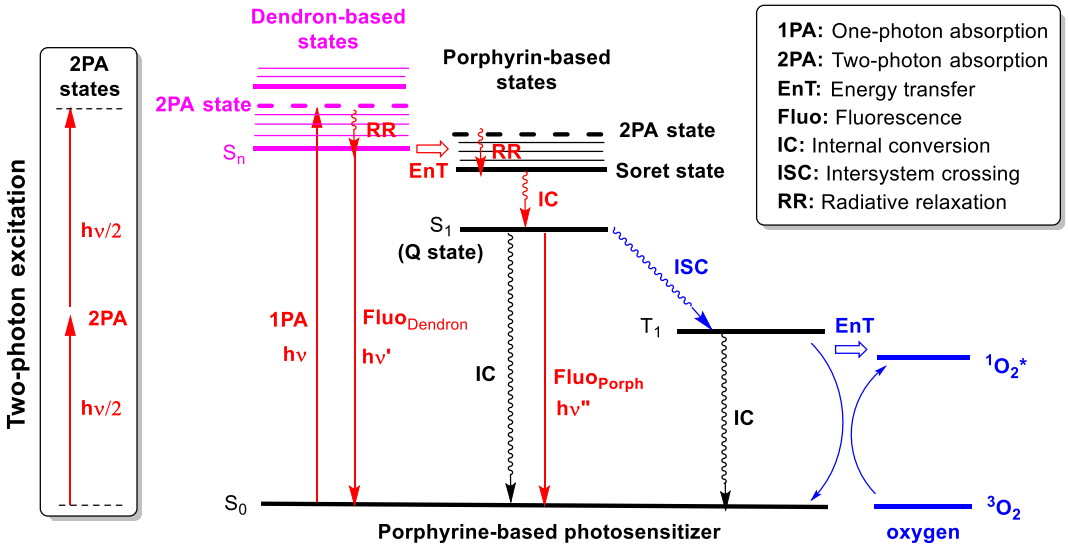

Scheme 10. Simplified Jablonski diagram showing the energy transfer and emissive processes following one-photon excitation in the dendron-based band for **1-8** (in red). The subsequent sensitization process of oxygen occurring from the lower triplet state after population of the porphyrin-based singlet Q state at lowest energy, is also sketched (in blue). The alternative two-photon excitation of these photosensitizers is shown on the left side.

Oxygen photosensitization. The quantum yields of singlet oxygen generation (Φ_Δ) were also determined for **1-8** (Table 2) and compared to that of the **TFP** free-base.[12] All new compounds exhibited higher Φ_Δ values, excepted for the Zn(II) complex **5** (57%), suggesting a similar or slightly improved tendency to photosensitize oxygen for the free-bases (**1-4**) than for **TFP**. Interestingly, metallation of any of these free-bases always slightly decreases its Φ_Δ value, suggesting that the increased intersystem crossing rate resulting from the presence of the Zn(II) ion (through the "heavy atom" effect), which already decreases its Φ_F, is also not beneficial to oxygen photosensitization.

Two-photon absorption (2PA). 2PA measurements were next conducted on the free-base porphyrins **1-4** in the near-IR range by two-photon excited fluorescence (TPEF) in CH_2Cl_2 (Figure 6a and Table 2). Although less fluorescent and less photoactive toward molecular oxygen, some of the Zn(II) complexes were also investigated by TPEF to evaluate the impact of metalation on their 2PA properties. Thus, both *generation-1* dendrimers **7** and **8**, as well as the compound **5**, formally corresponding to the *generation-0* dendrimer with C_{Tpa} connector were measured.

Table 2. Summary of 2PA properties of free-base porphyrins **1-4**, the Zn(II) complexes **5**, **7**, **8** and references in CH_2Cl_2.

Cmpd	λ_{2PA}^{max} (nm)	σ_2 [a] (GM)	Φ_F [b]	Φ_Δ [c]	$\sigma_2.\Phi_F^{max}$ (GM)	$\sigma_2.\Phi_\Delta^{max}$ (GM)
TFP	790	90	0.24	0.60	22	54
G'1	790	730	0.24	0.61	175	445
21	790	770	0.23	0.62	177	477
22	790	1450	0.17	0.46	247	667
23	790	840	0.12	0.40	101	336
1	830	780	0.21	0.70	164	546
2	790	590	0.20	0.68	118	401
3	810	1200	0.19	0.64	228	768
4	790	590	0.20	0.66	118	389
5	790	590	0.09	0.57	53	336
7	790	850	0.09	0.65	77	553
8	790	440	0.09	0.62	40	273

[a] Intrinsic 2PA cross-sections measured by TPEF in the femtosecond regime; a fully quadratic dependence of the fluorescence intensity on the excitation power is observed and 2PA responses are fully non-resonant. [b] Fluorescence quantum yield determined relative to tetraphenylporphyrin **TPP** in toluene.[c] Singlet oxygen formation quantum yield determined relative to **TPP** in dichloromethane (Φ_Δ[**TPP**] = 0.60).

For the free-bases, as expected, a significant increase of the 2PA cross-section compared to that of **TPP** (12 GM at 790 nm)[8] used as reference was observed for all porphyrins around 790-960 nm. In the *carbazole* series, the 2PA spectrum of the *first-generation* dendrimer (porphyrin **4**) is very similar to that of the *zero-generation* featuring carbazole as a simple donor group (porphyrin **2**). This clearly indicates that with such connectors, increasing the dendrimer generation is not a good way to obtain any significant improvement of the 2PA. In contrast, for the *triphenylamine* series (blue lines), we observe a significant improvement of the 2PA cross-section with increasing generation. Thus, σ_2^{max} = 780 GM for porphyrin **1** *vs.* σ_2^{max} = 1200 GM for porphyrin **3**. As this free-base porphyrin has the highest 2PA section cross-section of both series, it is the most promising model for developing luminescent 2PA-photosensitizers.

For the Zn(II) complexes (Figure 6b), the data reveals that metalation induces an overall decrease of the 2PA cross-sections above 700 nm compared to the free-bases, 20-25% lower values being found for σ_2^{max}. Among them, the zinc dendrimer **8** (corresponding to free-base **4**) exhibits the lowest 2PA cross-section of the series (440 GM).

Two-photon brightness. The combination of high fluorescence quantum yield (Φ_F) with high 2PA cross-section values (σ_2) leads to strong enhancements in the figures of merit of the two-photon action cross-section or two-photon brightness ($\Phi_F.\sigma_2$), which is the value classically used to estimate the performance of a given molecule for two-photon fluorescence imaging.[36] We first notice an increase along the *triphenylamine* series, this figure increases with *generation* upon going from compound **1** to **3** (164 to 228 GM), whereas no progression is seen for the *carbazole* series; no change from compound **2** to **4** (118 GM). Similar features are also observed for their Zn(II) complexes, but, given the large decrease in Φ_F and in σ_2^{max} observed after metallation, each of these derivatives has a lower value for the two-photon brightness ($\Phi_F.\sigma_2$) than its corresponding free-base. As a result, the *generation-1* porphyrin **3** presents the largest $\Phi_F.\sigma_2$ value (228 GM) and appears to be the best suited for two-photon fluorescence imaging.

Two-photon activation of oxygen. Likewise to $\Phi_F.\sigma_2$, $\Phi_\Delta.\sigma_2$ is the figure of merit classically used to evaluate oxygen-photosensitizing capability of a molecule after two-photon excitation (Table 2). Among the *triphenylamine* series, this figure increases with generation upon going from **1** to **3** (546 to 768 GM), whereas no progression is seen for the *carbazole* series; it decreases slightly from **2** to **4** (401 to 389 GM). Likewise to what was previously stated for the two-photon action cross-section, metalation by Zn(II) has no positive effect on this figure of merit compared to that of the corresponding free-bases. Again, the *generation-1* dendrimer **3** has the best two-photon oxygen sensitization cross-section (768 GM).

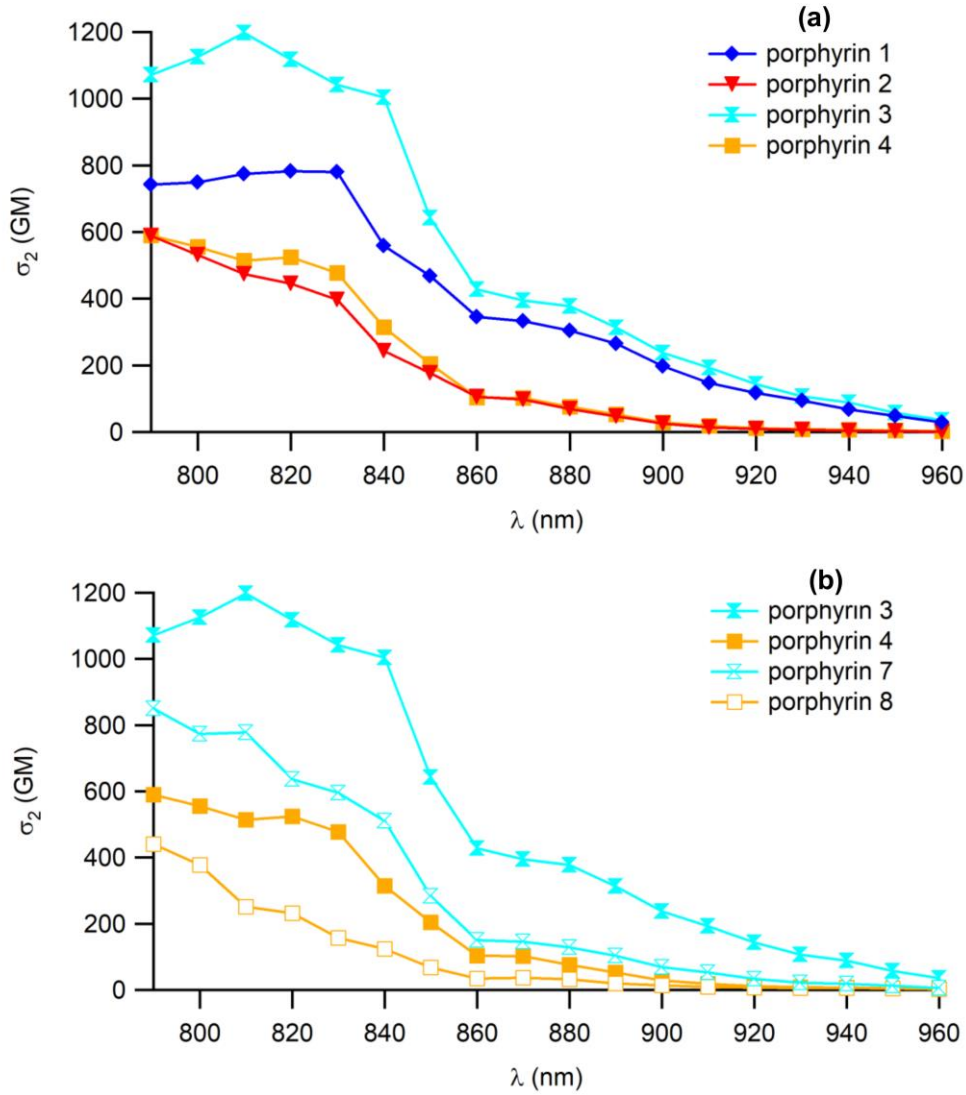

Figure 6. Two-photon absorption spectra of (a) free-base porphyrins,**1**-**4** and (b) comparison of free-base porphyrins **3**, **4** with corresponding zinc complexes **7** and **8**.

Discussion

At this point, among the various model compounds investigated in this contribution (**1**-**8**), we have shown that the *generation-1* free-base dendrimer **3** has the best figures of merit for two-photon imaging ($\Phi_F.\sigma_2^{max}$ = 228 GM) and for two-photon excited oxygen photosensitization ($\Phi_\Delta.\sigma_2^{max}$ = 768 GM). We have also shown that metallation by Zn(II) of any of the free-base porphyrins (**1**-**4**) had a detrimental effect on their fluorescence quantum yield, on their oxygen photosensitization quantum yield and on their two-photon absorption cross-section, making the corresponding Zn(II) complexes much less interesting for any theranostic applications. In the following, we will now briefly discuss the possible reasons for the better results obtained with the compounds featuring triarylamine connectors (C_{Tpa}) compared to their *N*-phenyl carbazole analogues (C_{Cbz}), given that molecular "rigidity" is often believed to contribute enhancing luminescence and 2PA cross-sections. Subsequently, we will compare these results obtained for the present compounds with those of their analogues previously investigated and featuring other connectors (C_{Ph}, C_{FluEt} and C_{FluAlk} described in Scheme 2) such as **G'1** (Scheme 1),[12] **20** or **21** (Scheme 11).[13]

Detrimental impact of metalation by Zn(II). The detrimental impact found on the the figures of merit for PDT after metalation of the free bases **1-4** by Zn(II) can appear surprising since conventional wisdom would suggest that due to the heavy atom effect, Zn(II) should favor intersystem crossing and thus should favor in turn PDT**.** While this is certainly so for many other tetrapyrrolic derivatives used in PDT such as tetraphenylporphyrin (**TPP**) or phthalocyanine, such an assumption rests on the belief that metalation will increase the intersystem crossing rate without notably affecting the non-radiative decay rate of the first triplet state and without notably affecting the oxygen photosensitizing rate nor the reactivity of the triplet state.[37] Our experimental data (Table 2) evidence that this is no more the case for **1-4** *vs.* **5-8**, perhaps because the tetrapyrrolic ring activating oxygen in these compounds is **TFP** and no more **TPP**, as also suggested by the fluorescence measurements (see below).

Impact of C_{Tpa} *vs.* C_{Cbz} connectors on the luminescence of these dendrimers. Then, when the luminescence quantum yields are considered for all these compounds along with their experimental uncertainties (± 5%), it appears that they are all the same for the either the free bases **1-4** or the Zn(II) complexes **5-8**, regardless the connector actually used in the peripheral dendrons or the generation considered. This is not so surprising considering that the emitting part of these fluorophores is essentially the central porphyrin ring, after intermolecular energy transfer has taken place from the peripheral arms. In this respect, for free-bases **1-4**, this quantum yield is also similar to that of isolated tetrafluorenylporphyrin (**TFP**) taken in the same solvent (Table 1). As expected, based on enhanced intersystem crossing (see above), the corresponding Zn(II) complexes present much lower luminescence quantum yields ($\Phi_F \approx 9\%$) but these are still significantly higher than that of **ZnTPP** often used as a reference ($\Phi_F = 3\%$).

Impact of C_{Tpa} *vs.* C_{Cbz} connectors on 2PA in dendrimers. When the absorption spectra of **1** and **2** are compared to that of the free-base **21** (Scheme 11),[12] used as reference for an extended star-shaped **TFP** porphyrin, we see that the maximum of the dendron-based absorption band in the latter compounds, at 370 and 343 nm, respectively (Table 1), is more red-shifted than that of **21** (339 nm). This indicate that, given of the smaller extension of the conjugated π-manifold directly conjugated with the peripheral fluorenyl groups of the central **TFP** in **1** and **2**, the charge transfer character (CT) induced by the electron releasing-substituent in these compounds during the transition is possibly the main reason of the red-shift of this band. As such, this red shift can be used to rank the electron-releasing character of the D_{Tpa} and D_{Cbz} donor groups in **1** and **2**. According to this spectroscopic marker, the D_{Tpa} endgroup appears significantly more electron-releasing than D_{Cbz} group. A similar conclusion about can be driven when the oxidation potentials of triphenylamine derivatives[38] and *N*-phenyl carbazoles[39] are considered. Actually, the nitrogen lone pair in *carbazole* contributes to the (aromatic) stabilization of the central five-membered ring and is therefore less available for delocalization on the *N*-aryl ring, resulting in a diminished electron-donation to the central **TFP** core compared to analogues featuring the C_{Tpa} connector instead (*i.e.* **1**, **3**, **5** and **7**).

This difference likely explains the larger 2PA cross-section found for **1** relative to **2**, since the D_{Tpa} endgroup will polarize more the peripheral arms than D_{Cbz} given the red-shift of the maxima in **1** compared to **2**. This larger arm-to-porphyrin CT character during the 2PA transition is a feature known to enhance the corresponding cross-sections.[4,22] Regarding 2PA, similar differences between D_{Tpa} and D_{Cbz} endgroups were already stated for dipolar two-photon absorbers featuring an identical acceptor group.[40] Likewise, when these units are now used as connectors in the free-bases porphyrins **3** and **4** after further extension of the π-manifold at their free *para*-phenyl positions, we state through the red-shift of the dendron-based band that the dendron extension is more effectively felt through *triphenylamine* connectors (C_{Tpa}) than through *carbazole* ones (C_{Cbz}). As a result, essentially the former compound (**3**) might experience a significant increase in the 2PA cross-section when moving from the *zero-generation* dendrimers (**1**, **2**) to the *first generation* (**3**, **4**). Similar statements can be made to rationalize the σ_2^{max} ordering of the corresponding Zn(II) complexes.

Then, when the 1PA spectra are plotted at twice their wavelength and overlaid with the corresponding 2PA spectra for all these compounds (ESI; Figures S18-19), we can notice that the 2PA maxima overlap more strongly with the dendron-based 1PA band in the case of compound **3** and **7**, suggesting that in this spectral range (around 800 nm), dendron-based 2PA states are also present in addition to porphyrin-based 2PA states. Keeping in mind that the maximum detected on the 2PA spectra results most likely from the simultaneous population of several closely-lying 2PA-allowed states, the red shift of the dendron-based 1PA band contributes here to significantly increase the density of excited states at the blue edge of the Soret band. This is also apparent on Scheme 10: upon lowering the energy of the first dendron-based excited states, more states become available for being populated by a 2PA transition at an energy just above that of the Soret band.

Thus, in spite of the enforced co-planarity of the C_{Cbz} spacer, [40] the more flexible C_{Tpa} spacer appears to be the best connector for favoring 2PA in these dendrimers. Besides the electronic factor discussed first which pertains to individual 2PA transitions, it seems that the red-shift of the dendron-based band might also contribute to increase their apparent 2PA cross-section via the "densification" of 2PA-allowed excited states present at lowest energy. This is certainly the case for **3** and **7**. After decaying, regardless their exact nature, all dendron-based excited states will eventually also populate S_1 via energy transfer and therefore contribute to sensitize oxygen (Scheme 10). Given that the difference between Φ_F and Φ_Δ for each set of *Tpa*- and *Cbz*-containing analogues is minimal, σ_2^{max} and λ_{2PA} become the main criteria for selecting the best two-photon photosensitizers among **1**-**8**. As a result, we find that by extending the π-manifold of **TFP** with 4-ethynyl-*N*,*N*-diphenylaniline groups (**1**), roughly the same σ_2^{max} value can be obtained than that previously obtained for the larger compound **21** (Scheme 11), but at a slightly more red-shifted wavelength (820 instead of 790 nm) and that, based on the classical figures of merit (Table 2), the free-base porphyrin **3** is the most promising photosensitizer among the new *generation-1* dendrimers presently tested (**3**, **4**, **7** and **8**).

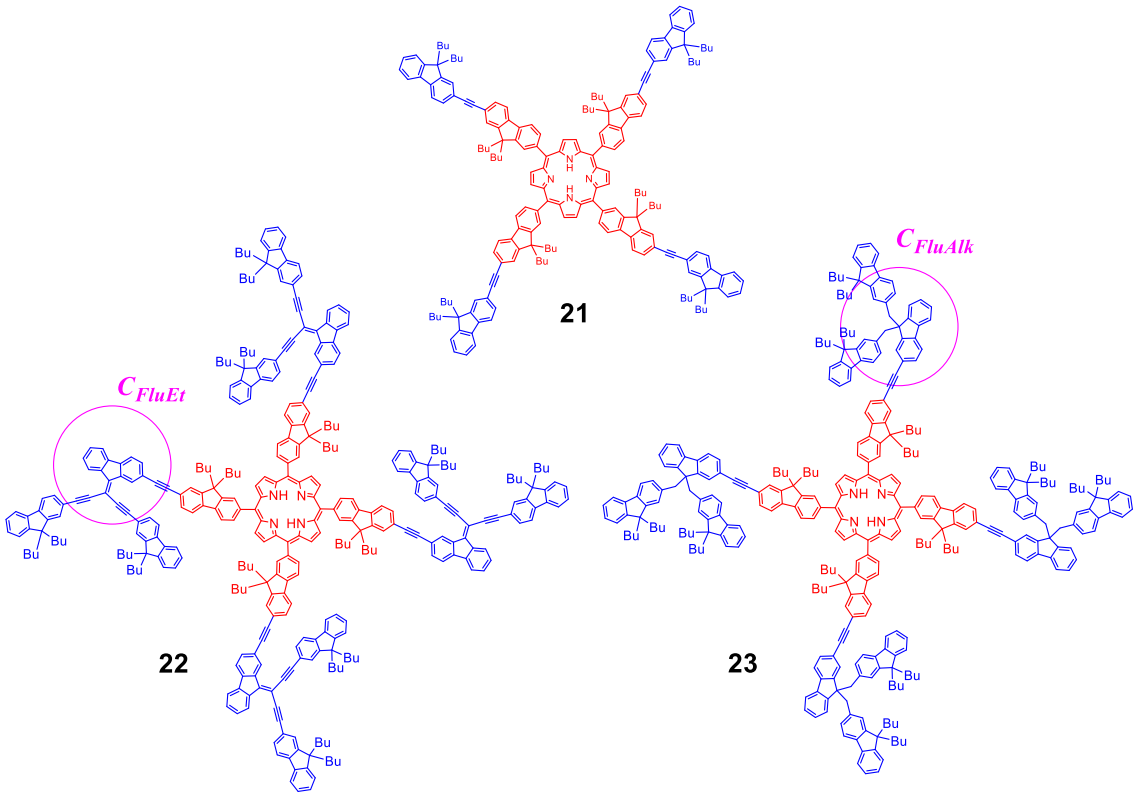

Scheme 11. Reference compound **21**[12] and dendrimeric analogues to **3** and **4** with C_{FluEt} (**22**) and C_{FluAlk} (**23**) connectors,[13] respectively.

Dendrimer 3 *vs.* other connectors previously studied. When the figures of merit of **3** are now compared to those of the previously described dendrimer ***G'1***, with a classic C_{Ph} connector (Scheme 1)[12] or to those of compounds **22** or **23**, which are analogues of ***G'1*** with other connectors,[13] we see that **3** is still the most promising photosensitizer for theranostics (Table 2). Indeed, among the latter compounds, only **22**, which possibly also benefits from a very red-shifted dendron-based band (see ESI; Figure S20), has a better σ_2^{max} value than **3**. However, this dendrimer presents lower Φ_F and Φ_Δ values, resulting in a slightly higher figure of merit for 2PA-imaging (228 *vs.* 247 GM; =8%), but in a much worse figure of merit for 2PA-PDT (768 *vs.* 667 GM; -15%). Furthermore, based on purely synthetic considerations only, **3** is also more easily available than **22**. In this respect, the free-base **1** certainly also corresponds to a quite promising two-photon photosensitizer for PDT provided both compounds can be water-solubilized.[41] Indeed, a quick comparison with figures of merit reported for other porphyrin-based systems independently reported two-photon photosensitization of oxygen reveal that compounds such as **1** or **3** would have some applied interest due to their comparably simpler structure. [7] These first results are therefore very encouraging to explore further the applied potential of these model compounds (or their water-soluble analogues) for theranostics and related medical uses.

Conclusions

In this work we have investigated the impact of changing the connectors C_n in **TFP**-cored dendrimers. First, the synthesis and characterization of two series of dendrimers having C_{Tpa} or C_{Cbz} junctions and of their zinc(II) complexes have been reported. In terms of photophysical properties, the new free-base porphyrins exhibit remarkably high luminescence quantum yields (≈ 20%), while these of their Zn(II) complexes are twice lower (around 9%). All these new porphyrins present good singlet oxygen photosensitization quantum yields (57 % ≤ Φ_Δ ≤ 70%), which are all higher than that of the reference **TFP** (Φ_Δ = 60%). Then, regarding their 2PA properties, the cross-sections for the *carbazole* derivatives **1** and **3** were independent of the dendrimer generation considered and slightly lower than that of the zero-generation dendrimer of the *triphenylamine* series (porphyrin **1**). However, a further and significant increase in the 2PA cross-section was observed (σ_2^{max} = 1200 GM) upon progressing to the first-generation dendrimer in the latter series (porphyrin **3**), showing that the size-limit for 2PA has not yet been reached, thus making these free-base porphyrins quite promising for developing new 2PA-photosensitizers for theranostics. Indeed, based on the relevant figures of merit, **3** presents both a comparably high two-photon brightness ($\Phi_F.\sigma_2^{max}$ = 228 GM) and the highest efficiency in two-photon singlet oxygen photosensitization ($\Phi_\Delta.\sigma_2^{max}$ = 768 GM) compared to analogous **TFP**-based dendrimers previously studied in the group. A rapid literarature survey reveals also that the new dendrimers **1** and **3** stand the comparison with many other single porphyrin systems independently reported for two-photon photosensitization of oxygen. These first results are therefore very encouraging to explore further the applied potential of these compounds and also of some water-soluble analogues for PDT, theranostics or related medical uses.

Experimental Section

Supplementary tables and figures are provided in the Supporting Information: Synthesis details, ^{1}H NMR and ^{13}C NMR characterization of all new compounds.

Materials. Compounds were purified by chromatography on silica gel using different mixtures of eluents as specified. Unless otherwise stated, all solvents used in reactions were distilled using common purification protocols, except DMF and ^{i}Pr$_2$NH which were dried on molecular sieves (3 Å). ^{1}H and ^{13}C NMR spectra were recorded on Bruker Ascend 400 and 500 at 298 K. The chemical shifts are referenced to internal tetramethylsilane (TMS). High-resolution mass spectra were recorded on different spectrometers: a Bruker MicrOTOF-Q II, a Thermo Fisher Scientific Q-Exactive in ESI positive mode and a Bruker Ultraflex III MALDI Spectrometer at CRMPO (Centre Regional de Mesures Physiques de l'Ouest) in Rennes. Reagents were purchased from commercial suppliers and used as received. The dendron precursors **10**,[12] **16**,[33] **17**,[33] **21**, **22**[12] and **27**[12] were obtained as previously described in the literature.

Synthesis. *Procedure for 9,9-dibutyl-7-((4-(diphenylamino)phenyl)ethynyl)-9H-fluorene-2-carbaldehyde (**9**).* In a Schlenk tube, a mixture of 4-ethynyl-*N*,*N*-diphenylaniline **13**[29] (0.3 g, 1.25 mmol, 1.5 eq), 7-bromo-9,9-dibutyl-9*H*-fluorene-2-carbaldehyde **14**[12] (0.3 g, 0.83 mmol, 1 eq), $PdCl_2(PPh_3)_2$ (26 mg, 0.037 mmol, 5% eq), CuI (7 mg, 0.037 mmol, 5% eq) was added into DMF (8 mL) and ^{i}Pr$_2$NH (8 mL) and was stirred at 100 °C for 48 hours under argon atmosphere. After cooling to room temperature, the solvents were evaporated and the residue was further purified by column chromatography (heptane/CH_2Cl_2 = 4/1, vol/vol), affording **9** as a yellow solid (452 mg, 95%). ^{1}H NMR (300 MHz, $CDCl_3$, ppm): δ 10.07 (s, 1H), 7.88-7.81 (m, 3H), 7.73 (d, *J* = 7.8 Hz 1H), 7.61-7.52 (m, 2H), 7.40 (d, *J* = 8.6 Hz, 2H), 7.32-7.29 (m, 3H), 7.14-7.00 (m, 9H), 2.08-1.97 (m, 4H), 1.15-1.03 (m, 4H), 0.67 (t, *J* = 7.3 Hz, 6H), 0.62-0.46 (m, 4H). ^{13}C NMR (75 MHz, $CDCl_3$, ppm): δ 192.2, 152.2, 151.8, 148.1, 147.2, 146.8, 139.4, 135.5, 132.6, 130.8, 130.6, 129.4, 126.0, 125.1, 123.8, 123.7, 123.1, 122.2, 120.9, 120.2, 115.8, 90.9, 89.4, 55.3, 40.0, 31.9, 29.0, 25.9, 23.0, 22.7, 14.1, 13.8. HRMS-ESI: m/z calcd for $C_{42}H_{39}NONa$: 596.29238; $[M+Na]^+$; found: 596.2924. Anal. Calcd. (%) for $C_{42}H_{39}NO$: C, 87.92; H, 6.85; N, 2.44. Found: C, 86.70; H, 6.80; N: 2.29.

*Procedure for 7-((4-(9H-carbazol-9-yl)phenyl)ethynyl)-9,9-dibutyl-9H-fluorene-2-carbaldehyde (**10**).* A mixture of 9-(4-bromophenyl)-9*H*-carbazole **15** (0.9 g, 2.91 mmol, 1.5 eq), 9,9-dibutyl-7-ethynyl-9*H*-fluorene-2-carbaldehyde **16**[33] (0.6 g, 1.94 mmol, 1 eq), $Pd(OAc)_2$ (10.5 mg, 0.049 mmol, 2.5% eq), CuI (18.6 mg, 0.097 mmol, 5% eq) and PPh_3 (25.5 mg, 0.097 mmol, 5% eq) in DMF (6 mL) and ^{i}Pr$_2$NH (6 mL) was stirred at 100 °C for 48 hours under argon atmosphere. After cooling to room temperature, the solvents were evaporated and the residue was further purified by chromatography (heptane/CH_2Cl_2 = 4/1, vol/vol), leading to the title compound as a yellow solid (560 mg, 51%). ^{1}H NMR (300 MHz, $CDCl_3$, ppm): δ 10.11 (s, 1H), 8.17 (d, *J* = 7.7 Hz, 2H), 7.95 (s, 1H), 7.91-7.80 (m, 5H), 7.67-7.61 (m, 4H), 7.51-7.44 (m, 4H), 7.37-7.32 (m, 2H), 2.16-2.03 (m, 4H), 1.21-1.09 (m, 4H), 0.76-0.57 (m, 10H). ^{13}C NMR (75 MHz, $CDCl_3$, ppm): δ 192.2, 152.3, 151.9, 146.7, 140.6, 140.0, 137.8, 135.7, 133.1, 131.0, 130.6,126.9, 126.2, 126.1, 123.6, 123.2, 123.1, 122.1, 121.0, 120.4,

120.4, 120.3, 109.7, 91.0, 89.8, 55.4, 40.0, 26.0, 23.0, 13.8. HRMS-ESI: m/z calcd for $C_{42}H_{37}NONa$: 594.27673; $[M+Na]^+$; found: 594.2767. Anal. Calcd. (%) for $C_{42}H_{37}NO$: C, 88.23; H, 6.52; N, 2.45. Found: C, 85.52; H, 6.43; N: 2.09.

Procedure for 7-((4-(bis(4-((9,9-dibutyl-9H-fluoren-2-yl)ethynyl)phenyl)amino) phenyl)ethynyl)-9,9-dibutyl-9H-fluorene-2-carbaldehyde (**11**). In a Schlenk tube, a mixture of bromo compound **17** (657 mg, 0.71 mmol, 1 eq), prepared 9,9-dibutyl-7-ethynyl-9H-fluorene-2-carbaldehyde **16** (469 mg, 1.42 mmol, 2 eq), $PdCl_2(PPh_3)_2$ (25 mg, 0.036 mmol, 5% eq) and CuI (6.8 mg, 0.036 mmol, 5% eq) was added in DMF (6 mL) and $^iPr_2NH$ (6 mL) under argon atmosphere. Then, the reaction was stirred at 100 °C for 48 hours. After cooling to room temperature, the solvents were evaporated and the residue was further purified by chromatography (heptane/CH_2Cl_2 = 7/2, vol/vol), affording the title compound as a yellow solid (524 mg, 63%). ^{1}H NMR (300 MHz, $CDCl_3$, ppm): δ 10.08 (s, 1H), 7.89-7.82 (m, 3H), 7.75 (d, J = 8.4 Hz, 1H), 7.72-7.67 (m, 4H), 7.58-7.49 (m, 12H), 7.38-7.31 (m, 6H), 7.11 (d, J = 8.6 Hz, 6H), 2.08-1.97 (m, 12H), 1.16-1.04 (m, 12H), 0.71-0.56 (m, 30H). ^{13}C NMR (75 MHz, $CDCl_3$, ppm): δ 192.2, 152.2, 151.8, 151.0, 150.8, 146.9, 146.8, 146.6, 141.4, 140.4, 139.6, 135.6, 132.8, 132.8, 130.8, 130.5, 127.5, 126.9, 126.1, 125.9, 124.2, 123.9, 123.6, 123.1, 122.9, 121.5, 120.9, 120.3, 120.0, 119.6, 118.3, 117.7, 90.6, 90.5, 90.0, 89.2, 55.3, 55.1, 40.2, 40.0, 31.9, 29.0, 25.9, 23.1, 23.0, 22.7, 14.1, 13.8. HRMS-MALDI: m/z calcd for $C_{88}H_{87}ON$: 1173.67822; $[M]^+$; found: 1173.6762. Anal. Calcd. (%) for $C_{88}H_{87}ON$: C, 89.98; H, 7.47; N, 1.19. Found: C, 89.24; H, 7.48; N, 0.96.

Procedure for 7-((4-(3,6-bis((9,9-dibutyl-9H-fluoren-2-yl)ethynyl)-9H-carbazol-9-yl)phenyl)ethynyl)-9,9-dibutyl-9H-fluorene-2-carbaldehyde (**12**). In a Schlenk tube, a mixture of compound **19** (0.5 g, 0.52 mmol, 1 eq), 9,9-dibutyl-7-ethynyl-9H-fluorene-2-carbaldehyde **16** (255 mg, 0.77 mmol, 1.5 eq), $PdCl_2(PPh_3)_2$ (18 mg, 0.026 mmol, 5% eq) and CuI (5 mg, 0.026 mmol, 5% eq) was added into DMF (6 mL) and $^iPr_2NH$ (6 mL) under argon atmosphere. Then the mixture was stirred at 100 °C for 48 hours. After cooling to room temperature, the solvents were evaporated and the residue was further purified by chromatography (heptane/CH_2Cl_2 = 2/1, vol/vol), giving the title compound as a red solid (205 mg, 33%). ^{1}H NMR (300 MHz, $CDCl_3$, ppm): δ 10.09 (s, 1H), 8.39 (d, J = 1.1 Hz, 2H), 7.91-7.80 (m, 6H), 7.73-7.69 (m, 5H), 7.67 (d, J = 1.5 Hz, 1H), 7.65-7.58 (m, 7H), 7.42 (d, J = 8.5 Hz, 2H), 7.39-7.32 (m, 6H), 2.13-1.99 (m, 12H), 1.17-1.05 (m, 12H), 0.73-0.49 (m, 30H). ^{13}C NMR (100 MHz, $CDCl_3$, ppm): δ 192.3, 152.3, 151.9, 151.0, 150.8, 146.6, 141.2, 140.5, 140.1, 136.8, 135.7, 133.3, 131.1, 130.6, 130.5, 130.1, 127.5, 136.9, 136.3, 125.9, 124.1, 123.3, 123.1, 123.0, 122.9, 121.8, 121.0, 120.4, 120.0, 119.7, 115.6, 110.1, 91.5, 90.2, 89.5, 55.4, 55.1, 40.3, 40.1, 26.0, 23.1, 23.0, 22.7, 13.9, 13.8. HRMS-MALDI: m/z calcd for $C_{88}H_{85}NO$: 1171.66257; $[M]^+$; found: 1171.656. Anal. Calcd. (%) for $C_{88}H_{85}NO$: C, 90.13; H, 7.31; N, 1.19. Found: C, 89.31; H, 7.51; N: 1.14.

*Procedure for free-base porphyrin **1**.* In a Schlenk tube, boron trifluoride etherate (25 μL) was added to a solution of aldehyde **9** (450 mg, 0.78 mmol, 1 eq) and pyrrole (67 μL, 0.78 mmol, 1 eq) in $CHCl_3$ (120 mL) under an argon atmosphere and the solution was stirred for 4 hours at room temperature. DDQ (133 mg, 0.59 mmol, 75% eq) was added and stirring was continued for an additional hour. The solvent was evaporated and the residue was purified by column chromatography (heptane/CH_2Cl_2 = 1/1, vol/vol) to furnish **1** as a purple powder (202 mg, 42%). ^{1}H NMR (400 MHz, $CDCl_3$, ppm): δ 8.91 (s, 8H), 8.24-8.19 (m, 8H), 8.06 (d, *J* = 7.3 Hz, 4H), 8.00-7.98 (m, 4H), 7.86 (d, *J* = 8.1 Hz, 8H), 7.79-7.73 (m, 8H), 7.63 (d, *J* = 8.2 Hz, 8H), 7.91 (d, *J* = 7.5 Hz, 4H), 7.65-7.63 (m, 8H), 7.45 (d, *J* = 8.4 Hz, 8H), 7.32-7.28 (m, 12H), 7.14 (d, *J* = 7.8 Hz, 16H), 7.10-7.04 (m, 20H), 2.23-2.07 (m, 16H), 1.26-1.16 (m, 16H), 0.99-0.87 (m, 16H), 0.80-0.74 (m, 24H), -2.57 (s, 2H). ^{13}C NMR (75 MHz, $CDCl_3$, ppm): δ 151.3, 149.6, 147.9, 147.3, 141.4, 141.0, 140.2, 133.8, 132.6, 130.9, 129.4, 126.1, 125.0, 123.6, 122.4, 122.3, 120.8, 120.1, 118.2, 116.3, 90.1, 89.8, 55.4, 40.3, 26.4, 23.2, 14.0. HRMS-MALDI: m/z calcd for $C_{184}H_{163}N_8$: 2484.29952; $[M+H]^+$; found: 2484.330. Anal. Calcd. (%) for $C_{184}H_{162}N_8{\cdot}CH_2Cl_2$: C, 86.45; H, 6.43; N, 4.36. Found: C, 86.75; H, 6.40; N, 4.15.

*Procedure for free-base porphyrin **2**.* In a Schlenk tube, boron trifluoride etherate (22 μL) was added to a solution of aldehyde **10** (400 mg, 0.70 mmol, 1 eq) and pyrrole (60 μL, 0.70 mmol, 1 eq) in $CHCl_3$ (100 mL) under argon atmosphere. The mixture was stirred for 4 hours at room temperature. DDQ (120 mg, 0.525 mmol, 75% eq) was added and stirring was continued for an additional hour. The solvent was evaporated and the residue was purified by column chromatography (heptane/CH_2Cl_2 = 1/1, vol/vol), leading to **2** as a purple powder (190 mg, 44%). ^{1}H NMR (400 MHz, $CDCl_3$, ppm): δ 8.95 (s, 8H), 8.27-8.23 (m, 8H), 8.18-8.12 (m, 12H), 8.00-7.98 (m, 4H), 7.86 (d, *J* = 8.1 Hz, 8H), 7.79-7.73 (m, 8H), 7.63 (d, *J* = 8.2 Hz, 8H), 7.51-7.44 (m, 16H), 7.33 (t, *J* = 7.0 Hz, 8H), 2.20-1.99 (m, 16H), 1.11-0.92 (m, 16H), 0.82-0.58 (m, 40H), -2.54 (s, 2H). ^{13}C NMR (100 MHz, $CDCl_3$, ppm): δ 151.4, 149.6, 141.5, 140.6, 140.1, 137.6, 133.8, 133.1, 131.1, 129.6, 126.9, 126.3, 126.1, 126.0, 123.6, 122.5, 121.7, 120.7, 120.4, 120.3, 120.1, 118.3, 109.8, 91.6, 89.1, 55.5, 53.4, 40.3, 31.9, 29.7, 26.4, 23.2, 22.7, 14.0. HRMS-MALDI: m/z calcd for $C_{184}H_{155}N_8$: 2476.23692; $[M+H]^+$; found: 2476.245. Anal. Calcd. (%) for $C_{184}H_{154}N_8{\cdot}CH_2Cl_2$: C, 86.72; H, 6.14; N, 4.37. Found: C, 87.58; H, 6.13; N, 4.16.

*Procedure for free-base porphyrin **3**.* In a Schlenk tube, boron trifluoride etherate (7.2 μL) was added to a solution of aldehyde **11** (270 mg, 0.23 mmol, 1 eq) and pyrrole (17 μL, 0.23 mmol, 1 eq) in $CHCl_3$ (20 mL) under an argon atmosphere, and the mixture was stirred for 4 hours at room temperature. DDQ (39 mg, 0.173 mmol, 75% eq) was added and

stirring was continued for another 1 hour. The solution was evaporated and the residue was purified by column chromatography (heptane/CH_2Cl_2 = 1/1, vol/vol), leading to the title compound as a purple powder (78 mg, 28%). ^{1}H NMR (400 MHz, $CDCl_3$, ppm): δ 8.94 (s, 8H), 8.26-8.22 (m, 8H), 8.08 (d, J = 7.2 Hz, 4H), 7.94 (d, *J* = 7.8 Hz, 4H), 7.72-7.67 (m, 24H), 7.56-7.51 (m, 40H), 7.37-7.31 (m, 26H), 7.16-7.13 (m, 22H), 2.18 (s, 16H), 2.02-1.98 (m, 32H), 1.27-1.06 (m, 48H), 0.82-0.56 (m, 120H), -2.56 (s, 2H). ^{13}C NMR (100 MHz, $CDCl_3$, ppm): δ 151.0, 150.8, 149.6, 146.7, 141.4, 141.2, 140.5, 140.1, 133.8, 132.8, 132.8, 130.5, 127.5, 126.9, 125.9, 124.1, 122.9, 122.0, 121.5, 120.7, 120.1, 120.0, 119.6, 118.2, 118.1, 118.0, 90.5, 89.3, 55.4, 55.1, 40.2, 26.4, 25.9, 23.1, 14.0, 14.0, 13.8. HRMS-MALDI: m/z calcd for $C_{368}H_{354}N_8$: 4884.79411; $[M]^+$; found: 4884.748. Anal. Calcd. (%) for $C_{368}H_{354}N_8$: C, 90.41; H, 7.30; N, 2.29. Found: C, 89.68; H, 7.14; N, 1.96.

*Procedure for free-base porphyrin **4***. In a Schlenk tube, boron trifluoride etherate (5.3 μL) was added to a solution of aldehyde **12** (200 mg, 0.17 mmol, 1 eq) and pyrrole (12.4 μL, 0.17 mmol, 1 eq) in $CHCl_3$ (15 mL) under argon atmosphere and the solution was stirred for 4 hours at room temperature. DDQ (29 mg, 0.13 mmol, 75% eq) was added and stirring was continued for another 1 hour. The solvent was evaporated and the residue was purified by column chromatography (heptane/CH_2Cl_2 = 1/1, vol/vol), leading to the title compound as a purple powder (75 mg, 36%). ^{1}H NMR (300 MHz, $CDCl_3$, ppm): δ 8.96 (s, 8H), 8.41 (s, 8H), 8.30-8.25 (m, 8H), 8.13 (d, *J* = 7.3 Hz, 4H), 7.99 (d, *J* = 7.9 Hz, 4H), 7.88 (d, *J* = 8.3 Hz, 8H), 7.77-7.59 (m, 44H), 7.45 (d, *J* = 8.4 Hz, 12H), 7.39-7.32 (m, 32H), 2.22-2.00 (m, 48H), 1.16-1.06 (m, 48H), 0.73-0.50 (m, 120H), -2.52 (s, 2H). ^{13}C NMR (75 MHz, $CDCl_3$, ppm): δ 151.5, 151.1, 150.8, 149.7, 141.7, 141.6, 141.3, 140.6, 140.1, 136.7, 133.9, 133.3, 130.6, 130.2, 127.5, 126.9, 126.3, 125.9, 124.1, 123.3, 123.2, 122.9, 121.8, 121.6, 120.8, 120.0, 119.7, 115.7, 110.2, 92.0, 90.3, 89.5, 88.9, 55.5, 55.1, 53.4, 40.3, 26.4, 26.0, 23.1, 14.1, 14.0, 13.9. HRMS-MALDI: m/z calcd for $C_{368}H_{346}N_8$: 4876.73151; $[M]^+$; found: 4876.738. Anal. Calcd. (%) for $C_{368}H_{346}N_8$: C, 90.56; H, 7.15; N, 2.30. Found: C, 89.84; H, 6.91; N, 2.07.

*Procedure for zinc porphyrin **5***. Free-base porphyrin **1** (90 mg, 0.036 mmol, 1 eq) and $Zn(OAc)_2$ (27 mg, 0.15 mmol, 4 eq) were dissolved in a mixture of DCM (20 mL) and MeOH (10 mL). The solution was stirred for 12 hours at 45 °C under argon atmosphere. After cooling to room temperature, the solvents were evaporated and the residue was further purified by recrystallization (DCM/MeOH = 1/15-20, vol/vol), affording **5** as a red powder (67 mg, 72%). ^{1}H NMR (300 MHz, $CDCl_3$, ppm): δ 9.04 (s, 8H), 8.34-8.15 (m, 8H), 8.07 (d, *J* = 7.4 Hz, 4H), 7.92 (d, *J* = 7.8 Hz, 4H), 7.64 (d, *J* = 6.9 Hz, 8H), 7.46 (d, *J* = 8.3 Hz, 8H), 7.33-7.28 (m, 12H), 7.17-7.05 (m, 36H), 2.32-2.06 (m, 16H), 1.23-1.18 (m, 16H), 1.00-0.75 (m, 40H). ^{13}C NMR (75 MHz, $CDCl_3$, ppm): δ 151.3, 150.4, 149.4, 147.9, 147.3, 141.9, 141.1, 139.4, 133.6, 132.6, 132.0, 130.8, 129.4, 126.0, 125.0, 123.6, 122.4, 122.2, 121.8, 120.0, 118.0, 116.3, 90.0, 89.8, 55.4, 40.3, 26.4, 23.2, 23.1, 14.0. HRMS-MALDI: m/z calcd for $C_{184}H_{160}N_8Zn$: 2545.20519; $[M]^+$; found: 2545.207. Anal. Calcd. (%) for $C_{184}H_{160}N_8Zn{\cdot}2CH_2Cl_2$: C, 82.18; H, 6.08; N, 4.12. Found: C, 81.82; H, 5.82; N, 3.84.

*Procedure for zinc porphyrin **6***. Free-base porphyrin **2** (80 mg, 0.032 mmol, 1 eq) and $Zn(OAc)_2$ (24 mg, 0.13 mmol, 4 eq) were dissolved in a mixture of DCM (20 mL) and MeOH (10 mL) under an argon atmosphere. The solution was stirred 12 hours at 45 °C. After cooling to room temperature, the solvents were evaporated and the residue was further purified by recrystallization (DCM/MeOH = 1/15-20, vol/vol), affording **6** as a red powder (76 mg, 93%). ^{1}H NMR (300 MHz, $CDCl_3$, ppm): δ 9.05 (s, 8H), 8.32-8.23 (m, 8H), 8.17-8.074 (m, 12H), 8.01-7.96 (m, 4H), 7.85 (d, *J* = 7.8 Hz, 8H), 7.78-7.72 (m, 8H), 7.62 (d, *J* = 8.0 Hz, 8H), 7.54-7.41 (m, 16H), 7.34-7.31 (m, 8H), 2.25-1.95 (m, 16H), 1.08-0.94 (m, 16H), 0.82-0.60 (m, 40H). ^{13}C NMR (100 MHz, $CDCl_3$, ppm): δ 151.4, 150.4, 149.4, 142.2, 141.6, 140.6, 137.5, 133.6, 133.1, 132.0, 131.1, 126.9, 126.2, 126.1, 123.6, 122.5, 121.6, 120.4, 120.2, 120.1, 120.1, 118.2, 109.9, 109.8, 91.6, 89.0, 55.4, 40.4, 40.2, 29.7, 26.4, 23.2, 22.4, 14.1, 14.0. HRMS-MALDI: m/z calcd for $C_{184}H_{152}N_8Zn$: 2537.14259; $[M]^+$; found: 2537.110. SLM 268. Anal. Calcd. (%) for $C_{184}H_{152}N_8Zn{\cdot}2CH_2Cl_2$: C, 82.42; H, 5.80; N, 4.13. Found: C, 81.71; H, 5.74; N, 3.90.

*Procedure for zinc porphyrin **7***. Free-base porphyrin **3** (50 mg, 0.01 mmol, 1 eq) and $Zn(OAc)_2$ (7.5 mg, 0.04 mmol, 4 eq) were dissolved into a mixture of DCM (12 mL) and MeOH (6 mL) under argon atmosphere. The solution was stirred for 12 hours at 45 °C. After cooling to room temperature, the solvents were evaporated and the residue was further purified by recrystallization (DCM/MeOH = 1/15-20, vol/vol), affording **7** as a red powder (42 mg, 82%). ^{1}H NMR (300 MHz, $CDCl_3$, ppm): δ 9.04 (s, 8H), 8.26-8.21 (m, 8H), 8.08 (d, J = 7.2 Hz, 4H), 7.94 (d, *J* = 7.8 Hz, 4H), 7.70-7.67 (m, 24H), 7.56-7.52 (m, 40H), 7.40-7.35 (m, 26H), 7.16-7.13 (m, 22H), 2.17-1.97 (m, 48H), 1.27-1.04 (m, 48H), 0.83-0.59 (m, 120H). ^{13}C NMR (75 MHz, $CDCl_3$, ppm): δ 151.3, 151.0, 150.8, 150.4, 146.7, 141.4, 140.5, 132.8, 130.5, 127.5, 126.9, 125.9, 124.1, 122.9, 121.5, 120.0, 119.6, 118.2, 118.1, 90.5, 89.3, 55.4, 55.1, 53.4, 40.2, 25.9, 23.2, 23.1, 14.0, 13.8. HRMS-MALDI: m/z calcd for $C_{368}H_{352}N_8Zn$: 4946.70815; $[M]^+$; found: 4946.640. Anal. Calcd. (%) for $C_{368}H_{352}N_8Zn{\cdot}2CH_2Cl_2$: C, 86.76; H, 7.01; N, 2.19. Found: C, 86.93; H, 6.83; N, 2.01.

*Procedure for zinc porphyrin **8***. Free-base porphyrin **4** (50 mg, 0.01 mmol, 1 eq) and $Zn(OAc)_2$ (7.5 mg, 0.04 mmol, 4 eq) were dissolved in a mixture of DCM (12 mL) and MeOH (6 mL) under an atmosphere of argon. The mixture was stirred for one day at 45 °C. After cooling to room temperature, the solvents were evaporated and the residue was further purified by recrystallization (DCM/MeOH = 1/15-20, vol/vol), affording **8** as a red powder (39 mg, 77%). ^{1}H NMR (300

MHz, $CDCl_3$, ppm): δ 9.07 (s, 8H), 8.41 (s, 8H), 8.31-8.28 (m, 4H), 8.17-8.12 (m, 4H), 8.04-7.99 (m, 4H), 7.93-7.88 (m, 8H), 7.78-7.59 (m, 48H), 7.47-7.44 (m, 12H), 7.32-7.27 (m, 32H), 2.22-2.02 (m, 48H), 1.25-1.11 (m, 48H), 0.83-0.71 (m, 120H), ^{13}C NMR (75 MHz, $CDCl_3$, ppm): δ 152.7, 151.0, 150.8, 150.4, 141.2, 140.5, 136.7, 134.3, 133.7, 133.3, 132.0, 130.5, 130.1, 127.5, 127.5, 127.0, 126.9, 126.9, 125.9, 124.1, 123.8, 123.3, 123.2, 122.9, 122.5, 121.9, 121.8, 121.5, 120.7, 120.5, 120.0, 119.7, 115.6, 110.2, 90.3, 89.5, 55.1, 40.26, 26.0, 23.1, 14.1, 14.0, 13.8. HRMS-MALDI: m/z calcd for $C_{368}H_{344}N_8Zn$: 2469.32223; $[M]^{2+}$; found: 2469.3232. Anal. Calcd. (%) for $C_{368}H_{344}N_8Zn{\cdot}2CH_2Cl_2$: C, 86.90; H, 6.86; N, 2.19. Found: C, 87.81; H, 6.81; N, 2.00.

Spectroscopic Measurements. All photophysical properties have been performed with freshly-prepared air-equilibrated solutions at room temperature (298 K). UV-Vis absorption spectra were recorded on a BIO-TEK instrument UVIKON XL spectrometer or on a Jasco V-570 spectrophotometer in THF (HPLC grade). Steady-state fluorescence measurements were performed on dilute solutions (*ca.* 10^{-6} M, optical density < 0.1) contained in standard 1 cm quartz cuvettes using an Edinburgh Instrument (FLS920) spectrometer in photon-counting mode. Fully corrected emission spectra were obtained, for each compound, after excitation at the wavelength of the absorption maximum, with $A_{\lambda ex}$ < 0.1 to minimize internal absorption.[42,43]

Measurements of singlet oxygen quantum yields (Φ_Δ). Measurements were performed on a Fluorolog-3 (Horiba Jobin Yvon), using a 450W Xenon lamp, with air-equilibrated solutions. The optical density of the reference and the sample solution were set equal to 0.15 at the excitation wavelength (maximum of the Soret band). The emission at 1272 nm was detected using a liquid nitrogen-cooled Ge-detector model (EO-817L). The emission spectra were corrected for the wavelength dependence of the lamp intensity and the excitation monochromator efficiency (excitation correction). Singlet oxygen quantum yields Φ_Δ were determined in dichloromethane solutions, using tetraphenylporphyrin (**TPP**) in dichloromethane as reference solution (Φ_Δ [**TPP**] = 0.60) and were estimated from $^1O_2$ luminescence at 1272 nm. The uncertainty of the values of the singlet oxygen quantum yields determined by this method was estimated to be ±0.05.

Two-Photon Absorption Experiments. To span the 790-920 nm range, a Nd:YLF-pumped Ti:sapphire oscillator (Chameleon Ultra, Coherent) was used generating 140 fs pulses at a 80 MHz rate. The excitation power is controlled using neutral density filters of varying optical density mounted in a computer-controlled filter wheel. After five-fold expansion through two achromatic doublets, the laser beam is focused by a microscope objective (10×, NA 0.25, Olympus, Japan) into a standard 1 cm absorption cuvette containing the sample. The applied average laser power arriving at the sample is typically between 0.5 and 40 mW, leading to a time-averaged light flux in the focal volume on the order of 0.1–10 mW/mm^2. The fluorescence from the sample is collected in epifluorescence mode, through the microscope objective, and reflected by a dichroic mirror (Chroma Technology Corporation, USA; ''red'' filter set: 780dxcrr). This makes it possible to avoid the inner filter effects related to the high dye concentrations used (10^{-4}M) by focusing the laser near the cuvette window. Residual excitation light is removed using a barrier filter (Chroma Technology; ''red'': e750sp–2p). The fluorescence is coupled into a 600 μm multimode fiber by an achromatic doublet. The fiber is connected to a compact CCD-based spectrometer (BTCCBZ12-E, B&WTek), which measures the two-photon excited emission spectrum. The emission spectra are corrected for the wavelength-dependence of the detection efficiency using correction factors established through the measurement of reference compounds having known fluorescence emission spectra. Briefly, the set-up allows for the recording of corrected fluorescence emission spectra under multiphoton excitation at variable excitation power and wavelength. 2PA cross sections (σ_2) were determined from the two-photon excited fluorescence (TPEF) cross sections ($\sigma_2.\Phi_F$) and the fluorescence emission quantum yield (Φ_F). TPEF cross sections of 10^{-4}M THF solutions were measured relative to fluorescein in 0.01 M aqueous NaOH using the well-established method described by Xu and Webb[44] and the appropriate solvent-related refractive index corrections.[45] The quadratic dependence of the fluorescence intensity on the excitation power was checked for each sample and all wavelengths.

ASSOCIATED CONTENT

Supporting Information: Supplementary tables and figures are provided in the Supporting Information: ^1H NMR and ^{13}C NMR characterization of all new compounds; retrosynthetic analysis and synthesis of various precursor compounds and also additional data on energy transfer and 2PA.

Acknowledgments: The authors acknowledge CNRS for their financial support and the China Scholarship Council (CSC) for PhD funding (LMS, ZS). This project was supported by the departmental committees CD35 of the "*Ligue contre le Cancer du Grand-Ouest*". We also thank Guillaume Clermont (ISM) for his help in the two-photon and singlet oxygen measurements.

References

1. Szacilowski, K. Digital Information Processing in Molecular Systems. *Chem. Rev.* **2008**, *108*, 3481-3548.
2. Wasielewski, M. R. Energy, Charge, and Spin Transport in Molecules and Self-Assembled Nanostructures Inspired by Photosynthesis. *J. Org. Chem.* **2006**, *71*, 5051-5060.
3. Josefsen, L. B.; Boyle, R. W. Unique Diagnostic and Therapeutic Roles of Porphyrins and Phthalocyanines in Photodynamic Therapy, Imaging and Theranostics. *Theranostics* **2012**, *2*, 916-966.
4. 4. Pawlicki, M.; Collins, H. A.; Denning, R. G.; Anderson, H. L. Two-Photon Absorption and the Design of Two-Photon Dyes. *Angew. Chem. Int. Ed.* **2009**, *48*, 3244-3266
5. Bhaumik, J.; Mittal, A. K.; Banerjee, A.; Chisti, Y.; Banerjee, U. C. Applications of phototheranostic nanoagents in photodynamic therapy. *Nano Res.* **2015**, *8*, 1373-1394.
6. Prabhu, P.; Patravale, V., The upcoming field of theranostic nanomedicine: an overview. *J. Biomed. Nanotechnol.* **2012**, *8*, 859-882.
7. Bolze, F.; Jenni, S.; Sour, A.; Heitz, V. Molecular photosensitisers for two-photon photodynamic therapy. *Chem. Commun.* **2017**, *53*, 12857-12877.
8. Mongin, O.; Hugues, V.; Blanchard-Desce, M.; Merhi, A.; Drouet, S.; Yao, D.; Paul-Roth, C. Fluorenyl porphyrins for combined two-photon excited fluorescence and photosensitization. *Chem. Phys. Lett.* **2015**, *625*, 151–156.
9. Drouet, S.; Paul-Roth, C. O.; Simonneaux, G. Synthesis and photophysical properties of porphyrins with fluorenyl pendant arms. *Tetrahedron* **2009,** *65*, 2975-2981.
10. Drouet, S.; Paul-Roth, C. O., Fluorenyl Dendrimer Porphyrins: Synthesis and Photophysical Properties. *Tetrahedron* **2009,** *65*, 10693-10700.
11. Yao, D.; Zhang, X.; Mongin, O.; Paul, F.; Paul-Roth, C. O. Synthesis and Characterization of New Conjugated Fluorenyl-Porphyrin Dendrimers for Optics. *Chem. Eur. J.* **2016,** *22*, 5583-5597.
12. Yao, D.; Zhang, X.; Triadon, A.; Richy, N.; Mongin, O.; Blanchard-Desce, M.; Paul, F.; Paul-Roth, C. O., New Conjugated *meso*-Tetrafluorenylporphyrin-cored Derivatives as Fluorescent Two-photon Photosensitizers for Singlet Oxygen Generation. *Chem. Eur. J.* **2017**, *23*, 2635-2647.
13. Zhang, X.; Ben Hassine, S.; Richy, N.; Mongin, O.; Blanchard-Desce, M.; Paul, F.; Paul-Roth, C. O., New Porphyrin Dendrimers with Fluorenyl-based Connectors: A Simple Way to improving the Optical Properties over Dendrimers featuring 1,3,5-Phenylene Connectors. *New J. Chem.* **2020**, *44*, 4144-4157.
14. Paul-Roth, C. O.; Williams, J. A. G.; Letessier, J.; Simonneaux, G. New tetra-aryl and bi-aryl porphyrins bearing 5,15-related fluorenyl pendants: the influence of arylation on fluorescence. *Tetrahedron Lett.* **2007**, *48*, 4317-4322.
15. Varnavski, O.; Yan, X.; Mongin, O.; Blanchard-Desce, M.; Goodson, T. G., III, Strongly interacting organic conjugated dendrimers with enhanced two-photon absorption. J. Phys. Chem. C 2007, 111, 149-162.
16. Terenziani, F.; Katan, C.; Badaeva, E.; Tretiak, S.; Blanchard-Desce, M., Enhanced Two-Photon Absorption of Organic Chromophores: Theoretical and Experimental Assessments. *Adv. Mater.* **2008**, *20*, 4641-4678.
17. Wan, Y. ; Yan, L. ; Zhao, Z. ; Ma, X. ; Guo, Q. ; Jia, M.; Lu, P. ; Ramos-Ortiz, G. ; Maldonado, J. L.; Rodríguez, M.; Xia, A. Gigantic two-photon absorption cross sections and strong two-photon excited fluorescence in pyrene core dendrimers with fluorene/carbazole as dendrons and acetylene as linkages. *J. Phys. Chem. B.*, **2010**, *114*, 11737–11745.
18. Ding, J.; Zhang, B.; Lü, J.; Xie, Z.; Wang, L.; Jing, X.; Wang, F. Solution-processable carbazole-based conjugated dendritic hosts for power-efficient blue-electrophosphorescent devices. *Adv. Mater.*, **2009**, *21*, 4983–4986.
19. Zhao, Z.; Xu, X.; Chen, X.; Wang, X.; Lu, P.; Yu, G.; Liu, Y., Synthesis and Characterization of Deep Blue Emitters from Starburst Carbazole/Fluorene Compounds. *Tetrahedron* **2008**, *64* (11), 2658-2668.
20. Kannan, R.; He, G. S.; Yuan, L.; Xu, F.; Prasad, P. N.; Dombroskie, A. G.; Reinhardt, B. A.; Baur. J. W.; Vaia. R. A.; Tan, L. S. Diphenylaminofluorene-based two-photon-absorbing chromophores with various π-electron acceptors. *Chem. Mater.* **2001,** 13, 1896–1904.
21. Gautier, Y.; Argouarch, G.; Malvolti, F.; Blondeau, B.; Richy, N.; Amar, A.; Boucekkine, A.; Nawara, K.; Chlebowicz, K.; Orzanowska, G.; Matczyszyn, K.; Dudek, M.; Samoc, M.; Blanchard-Desce, M.; Mongin, O.; Waluk, J.; Paul, F., Triarylisocyanurate-Based Fluorescent Two-Photon Absorbers. *ChemPlusChem* 2020, 85, 411-425.
22. He, G. S.; Tan, L.-S.; Zheng, Q.; Prasad, P. N., Multiphoton Absorbing Materials: Molecular Designs, Characterizations, and Applications. *Chem. Rev.* **2008**, *108*, 1245-1330.
23. Joon Lee, G.; Kim, K.; Jin, J.-I., Mechanism of one- and two-photon absorption induced photoluminescence in PPV type, electroluminescent polymer. *Opt. Commun*. **2002**, *203*, 151-157.
24. Tamura, K.; Fujii, T.; Shiotsuki, M.; Sanda, F.; Masuda, T. Synthesis and properties of polyacetylenes having pendent phenylethynylcarbazolyl groups. *Polymer*, **2008**, *49*, 4494–4501.
25. Lindsey, J. S.; Hsu, H. C.; Schreiman, I. C. Synthesis of tetraphenylporphyrins under very mild conditions. *Tetrahedron Lett.* **1986**, *27*, 4969-4970.
26. Lindsey, J. S.; Schreiman, I. C.; Hsu, H. C.; Kearney, P. C.; Marguerettaz A. M. Synthesis of tetraphenylporphyrins under very mild conditions. *J. Org. Chem*., **1987**, *52*, 827-836.
27. Paul-Roth, C. O.; Simonneaux, G. Porphyrins with fluorenyl and fluorenone pendant arms. *C.R. Acad. Sci., Ser. IIb: Chim.* **2006,** 9, 1277-1286.

28. Shi, L.; He, C.; Zhu, D.; He, Q.; Li, Y.; Chen, Y.; Sun, Y.; Fu, D.; Wen, H.; Cao, J.; Cheng, J. High performance aniline vapor detection based on multi-branched fluorescent triphenylamine-benzothiadiazole derivatives: branch effect and aggregation control of the sensing performance. *J. Mater. Chem.*, **2012**, *22*, 11629-11635.
29. Li, Q.; Guo, H.; Ma, L.; Wu, W.; Liu, Y.; Zhao, J. Tuning the photophysical properties of N^ N Pt (II) bisacetylide complexes with fluorene moiety and its applications for triplet–triplet-annihilation based upconversion. *J. Mater. Chem.*, **2012**, *22*, 5319-5329.
30. Sonogashira, K.; Tohda, Y.; Hagihara, N. A convenient synthesis of acetylenes: catalytic substitutions of acetylenic hydrogen with bromoalkenes, iodoarenes and bromopyridines. *Tetrahedron Lett.*, **1975**, *16*, 4467-4470.
31. Pfoertner, K. H. "Photochemistry" in Ullmann's Encyclopedia of Industrial Chemistry, **2002**, Wiley-VCH, Weinheim.
32. Wu, M. S.; Tang, W. C. Dye Compound and Photoelectric Component Using the Same. US2010122729 (A1), May 20, **2010**.
33. Tian, Y.; Wu, W.; Chen, C.; Strovas, T. ; Li, Y.; Jin, Y.; Su, F. ; Meldrum, D. R.; Jen. . A. K. Y. 2,1,3-Benzothiadiazole (BTD)-moiety-containing red emitter conjugated amphiphilic poly(ethylene glycol)-block-poly(3-caprolactone) copolymers for bioimaging. *J. Mater. Chem.*, **2010**, *20*, 1728-1736.
34. Lu, W. E.; Dong, X. Z.; Chen, W. Q.; Zhao, Z. S.; Duan, X. M. Novel photoinitiator with a radical quenching moiety for confining radical diffusion in two-photon induced photopolymerization. *J. Mater. Chem.*, **2011**, *21*, 5650-5659
35. Cao, D.; Zhu, L.; Liu, Z.; Lin, W., Through bond energy transfer (TBET)-based fluorescent chemosensors. *J. Photochem. Photobiol. C* **2020,** *44*, 100371.
36. Kim, H. M.; Cho, B. R. Two-photon materials with large two-photon cross sections. Structure-property relationship. *Chem. Commun.* **2009,** *45*, 153-164.
37. Wilkinson, F.; Helman, W. P.; Ross, A. B., Quantum Yields for the Photosensitized Formation of the Lowest Electronically Excited Singlet State of molecular Oxygen in Solution. *J. Phys. Chem. Ref. Data* **1993**, 22, 113-262.
38. Yuan Chiu, K.; Xiang Su, T.; Hong Li, J.; Lin, T.-H.; Liou, G.-S.; Cheng, S.-H., Novel trends of electrochemical oxidation of amino-substituted triphenylamine derivatives. *J. Electroanal. Chem.* **2005**, 575, 95-101.
39. Karon, K.; Lapkowski, M., Carbazole electrochemistry: a short review. *J. Solid State Electrochem.* **2015**, 19, 2601-2610.
40. Cao, D.-X.; Fang, Q.; Wang, D.; Liu, Z.-Q.; Xue, G.; Xu, G.-B.; Yu, W.-T., Synthesis and Two-Photon-Excited Fluorescence of Benzothiazole-Based Compounds with Various π-Electron Donors. *Eur. J. Org. Chem.* **2003**, 3628-3636.
41. Shi, L.; Nguyen, C.; Daurat, M.; Richy, N.; Gary-Bobo, M.; Cammas-Marion, S.; Mongin, O.; Paul-Roth, C. O.; Paul, F., Encapsulation of hydrophobic porphyrins into biocompatible nanoparticles: an easy way to benefit of their two-photon photo-therapeutic effect without hydrophilic functionalization. *Cancers* **2022**, 14 (2358) and refs therein.
42. Demas, N.; Crosby, G. A. Measurement of photoluminescence quantum yields. *J. Phys. Chem.* **1971**, 75, 991-1024.
43. Eaton, G. R.; Eaton, S. S. EPR studies of long-range intramolecular electron-electron exchange interaction. *Acc. Chem. Res.* **1988**, 21, 107-113.
44. Xu, C.; Webb, W. W. Measurement of two-photon excitation cross sections of molecular fluorophores with data from 690 to 1050 nm. *J. Opt. Soc. Am. B* **1996,** 13, 481-491.
45. Werts, M. H. V.; Nerambourg, N.; Pélégry, D.; Le Grand, Y.; Blanchard-Desce, M. Action cross sections of two-photon excited luminescence of some Eu(III) and Tb(III) complexes. *Photochem. Photobiol. Sci.* **2005,** 4, 531-538.